NAL PROPOSAL No. 152

Scientific Spokesman:
C. A. Heusch
Division of Natural Sciences
University of California
Santa Cruz, California 95060

FTS/Off-net: 415 - 556-9000
408 -429-2333

Proposal
to Build an Electron-Photon Facility at NAL
and
to Measure Photon Scattering at High Energies

D. E. Dorfan, S. M. Flatté, C. A. Heusch, G. Luxton,
C. del Papa, and A. Seiden

July 18, 1971

UCSC - 005

July 18, 1971

Proposal

to Build an Electron-Photon Facility at NAL

and

to Measure Photon Scattering at High Energies

D.E. Dorfan, S.M. Flatté, C.A. Heusch, G. Luxton,

C. del Papa, and A. Seiden

Division of Natural Sciences, University of California

Santa Cruz, California 95060

Correspondent: C.A. Heusch
408-429-2333

TABLE OF CONTENTS

	Page
General Introduction	2
Physics Motivation	
$\sigma_{tot}(\gamma p)$ and $\sigma_{elastic}(\gamma p)$	5
$\sigma_{tot}(\gamma A)$	10
$\gamma p \rightarrow \gamma$ + hadrons	12
Electron - Photon Beam	16
Photon Tagging System	24
Measurement of Beam Energy and Angle	27
Detection System	29
Rates and Backgrounds	36
Running Time	42
Equipment and Personnel	44
References	45

General Introduction

The National Accelerator Laboratory opens up a new era in our search of what elementary particles are like; the 100-500 GeV era. If we want to look at the structure of hadrons with the resolution provided by the wavelength of such high energy beams, what can be more natural, to paraphrase Bjorken,[1)] than "looking" at them, i.e. shining light at them and watching for scattering or absorption ?

This is precisely what we propose to do in the experiments suggested here. Photons, real and virtual, have contributed immeasurably to our understanding of hadronic matter through investigations done at lower-energy ($1 \leq E \leq 20$ GeV) electron accelerators. NAL, albeit a proton machine, will be our only potential source of photons beyond SLAC energies. Proton-nucleus collisions will produce photons, principally in two-step processes involving radiative hadron (notably π^0) decays. It has been shown[2)] that sizeable fluxes can be obtained by the appropriate construction of beam lines.

NAL will then be a unique tool for the study of electromagnetic interactions at energies in the 20-300 GeV range. At high energies ($\gtrsim 200$ GeV), available electron fluxes will set the limit on photon intensities for experimentation; at lower energies, fluxes rise strongly, but the electronics logic involved in beam momentum definition and tagging will not permit final yields to be considerably larger than those at 200 GeV. The first generation of photon physics at NAL will therefore restrict itself to processes with relatively large cross-sections. As will be seen, some of the most exciting problems involving photons at presently existing energies will be accessible to conclusive experimentation at NAL.

Our group has, from past experience at lower-energy photon laboratories and from recent studies of its members, a keen interest in working on these problems. We have been happily active on earlier feasibility studies of beams and experiments;[3)] and we are enthusiastic about the prospect of a photon beam becoming available at NAL at an early date.

We propose to participate actively, as we have done in the past, in the design and implementation of the electron-photon facility, and to perform at the earliest possible date an experiment which will yield information on three vitally important processes in photon scattering:

1) measurement of the total hadronic photon cross-section on nucleons and nuclei;
2) elastic photon scattering (proton compton effect);
3) inelastic photon scattering;

as a byproduct, we will have data on yields of π^o, η^o, X^o, ω^o, ... through their 2γ or 3γ decay modes.

The set of experiments proposed here, together with experiments proposed by other groups, will tell us not only about the structure of the hadrons, but about the behavior of the photon at high energies. It has the virtue of being accessible through one basic, well-integrated set of experimental equipment, as detailed below.

The facility as well as the detection apparatus is being developed in consultation with the MIT - Canada collaboration. Equipment may be shared, and some of the running may be able to proceed compatibly. The success of this program will depend crucially on the design of appropriate halo-free beam lines; and on the early design and testing of optimal shower detection equipment - for both energy measurement and localization (or trajectory reconstruction). Our group has considerable experience in both these areas[4). Shower detectors are being built in Santa Cruz and can be conveniently tested at nearby SLAC. Also, a beam designed by our group, which we feel is flexible, economical, and viable, is included in this proposal.

The essential feature of our proposal is this: Our shower detection equipment can be tested and calibrated in available SLAC beams before the first turn-on of the NAL photon beam, and will be ready at that time. While information on the longitudinal and lateral shower spread can be extrapolated to NAL energies from existing data up to 15-20 GeV, the validity of such extrapolations must be experimentally tested at an early date. Together with the energy resolution to be expected at NAL energies, such data will vitally affect what can and what cannot be done: resolution of neighboring showers, recognition of radiative meson decays, total energy balance, etc. We feel therefore it is imperative that at the earliest possible date, an electron beam of high purity (if low-intensity) be available for the measurement of such parameters. Our equipment will be present, tested up to SLAC energies, when the first photon beam emerges.

Physics Motivation

I. $\sigma_{tot}(\gamma p)$ and $\sigma(\gamma p \to \gamma p)$

The relationship between the total cross-section and the forward scattering amplitude for γp interactions has long been a source of fundamental interest in particle physics. While similar relations have been well tested in πN scattering, photon-induced processes have not been checked with comparable accuracy. Quite apart from such relations, these basic cross-sections separately provide accessible information on hadron-photon analogies, as will be seen below.

Recall that the forward Compton scattering amplitude can be written:

$$f(\nu) = f_1(\nu)\vec{\varepsilon}_2^{\,*} \cdot \vec{\varepsilon}_1 + i\, f_2(\nu)\vec{\sigma} \cdot (\vec{\varepsilon}_2^{\,*} \times \vec{\varepsilon}_1)$$

where $\vec{\varepsilon}_1$ and $\vec{\varepsilon}_2$ are the polarization vectors of the initial and final photons, and ν is the laboratory energy of the incoming photon.

A. The Optical Theorem

We can write, for unpolarized states:

$$\sigma_{tot} = (4\pi/\nu)\,\mathrm{Im}\, f_1(\nu)$$

$$D(\nu) = \left(\frac{d\sigma}{dt}(\nu)\ (\gamma p \to \gamma p)\right)_{t=o} = \frac{\pi}{\nu^2}\left\{|f_1|^2 + |f_2|^2\right\}$$

Thus a measure of $\sigma_t(\nu)$ and $D(\nu)$ gives $\mathrm{Im}\, f_1(\nu)$ and $(\mathrm{Re} f_1(\nu))^2 + |f_2(\nu)|^2$.

B. The Forward Dispersion Relation

The oldest dispersion relation, derived by Gell-Mann, Goldberger and Thirring[5] as a fundamental consequence of locality and causality, can be written

$$\mathrm{Re} f_1(\nu) = f_1(o) + \frac{\nu^2}{\pi} P \int_{\nu_o}^{\infty} \frac{d\nu'^2}{\nu'^2 - \nu^2}\ \frac{\mathrm{Im} f_1(\nu')}{\nu'^2}$$

or

$$\mathrm{Re} f_1(\nu) = \frac{-\alpha}{M_N} + \frac{\nu^2}{2\pi^2} \int_{\nu_o}^{\infty} \frac{\sigma_{tot}(\nu')\,d\nu'}{\nu'^2 - \nu^2}$$

where $\nu_0 = m_\pi + m_\pi^2 / 2M_N$ (single-pion-production threshold). Thus our measurement of $\sigma_{tot}(\nu)$ will allow the determination of $\mathrm{Re}f_1(\nu)$ for large ν and we can then

1) determine $|f_2(\nu)|$, or set an upper limit. (Interest in $f_2(\nu)$ has been pointed out by Adler and Dashen[6]);

2) test the dispersion relation in the sense that measurement of $D(\nu)$ gives an upper bound on $\mathrm{Re}f_1(\nu)$ and measurement of $\sigma_{tot}(\nu)$ yields a value for $\mathrm{Re}f_1(\nu)$ which must be consistent with that upper bound.

C. Asymptotic Behavior.

We know that at $\nu = o$, $f(\nu)$ must be given by the Thomson value $-\frac{\alpha}{M_N}$. In other words

$$\mathrm{Re}f_1(o) = -\frac{\alpha}{M_N}, \quad \mathrm{Im}f_1(o) = 0.$$

An important question, raised by Creutz, Drell, and Paschos[7], is what happens to this term as $\nu \to \infty$? Does the contribution of strong interactions (multiparticle production) cancel this term? This question is directly related to a well-known paradox in Regge theory: If elastic scattering at high energy is mediated by the Pomeron, and the Pomeron has intercept $\alpha(o) = 1$ (i.e. it acts like a vector particle at $t = o$), then the forward Compton amplitude must vanish because a a vector particle cannot couple to two photons[8]. Experimentally, of course, it does not vanish at presently accessible energies, and we do not expect it to vanish at $\nu \to \infty$. Thus something other than the Pomeron contributes, or we don't understand the Pomeron. Is there a fixed pole at $J = 1$, or an additional moving pole? Either of these possibilities will have to be checked against whatever high-energy behavior we find.

Damashek and Gilman[9] fitted the known σ_t experimental data to a smooth function which at high energy has the form

$$\sigma_t(\nu) = a + b/\sqrt{\nu},$$

a form suggested by the Regge picture. They then derive a finite-energy sum rule for $\mathrm{Re}f_1(\nu)$ which gives

$$\mathrm{Re}f_1(\nu) \underset{\nu\to\infty}{\longrightarrow} \frac{b}{4\pi}\sqrt{\nu} - \frac{\alpha}{M_N} + A ,$$

where A is a contribution of strong interactions to the constant term. By using the dispersion relation to evaluate $\mathrm{Re}f_1(\nu)$, and finding b from $\sigma_t(\nu)$, they suggest that in fact $A \approx 0$, but the errors are too large to draw a firm conclusion yet. Clearly, as $\nu \to \infty$ the determination of A becomes harder. In fact our measurements, rather than determining A, will serve to measure b from $\sigma_t(\nu)=a+b/\sqrt{\nu}$. The above equation for $\mathrm{Re}f_1$ can then be evaluated at lower energies to yield a more reliable result for A.

D. Massive QED

It is no doubt of interest to see whether the only really successful theory of particle interactions (QED) can be carried over to the strong interaction case. In analyzing hadron-hadron interactions, Cheng and Wu[10] have studied all tower graphs contributing to the high energy limit, in analogy to QED. The detailed features of Cheng and Wu's work are, of course, dependent on their particular model. For the experimentalist, however, their work has the particular virtue of making definite predictions; the main physical ingredient is that there is, at asymptotic energies, total absorption of the incoming wave by a scatterer with logarithmically growing radius. It will be interesting to check the implications of this picture:

(1) $\dfrac{\mathrm{Re}\ f(o)}{\mathrm{Im}\ f(o)} \longrightarrow o$ (logarithmically with energy);

(2) $\dfrac{\sigma_{el}}{\sigma_{tot}} \approx \frac{1}{2}$ + (terms $\to$ o, logarithmically with energy);

(3) $\sigma_{tot}(s) \to (\log s)^2$;

(4) $\dfrac{d\sigma}{dt}$ has minima at predicted locations.

How far can the analogy to QED be carried? For hadrons, hadron scattering will tell. For photons, is there such a pattern observable ? The hadronic character of the photon is again on the line. We note that first ISR results indicate that $\frac{\sigma_{el}}{\sigma_{tot}}$, at energies reached there, is $\simeq \frac{1}{6}$, instead of the asymptotic predictions of Rule (2). Moreover, this rule will obviously be suppressed by $\sim\frac{1}{137}$ on the RHS, for the photonic final state.

Cheng and Wu[11] recently reviewed their predictions for photon-induced processes and find that, in their impact description, the proton looks like a gray disk to photons (transparent to the bare photon, black to the hadronic part). The scattering amplitude is then proportional to $\frac{R}{\Delta} J_1 (R\,\Delta)$, with R the expanding radius, Δ the momentum transfer: at NAL, we should find the first dip in the Bessel function with acceptable counting rates between $t = 1$ and $2\ (\mathrm{GeV}/C)^2$, if their model is correct.

E. Vector Meson Dominance Model

The Quark Model

If the photon acts approximately like a ρ meson (VMD), it is expected to behave like other $q\,\bar{q}$ states, as long as we can take the quark model for crude guidance. Present data indeed show a striking similarity between the energy trend of $\sigma_{tot}\ (\gamma p)$ and $\frac{1}{2}\left[\sigma_{tot}\ (\pi^+ p) + \sigma_{tot}\ (\pi^- p)\right]$, when normalized at low energies[12]. Will this similarity continue at very high energies ?

High Energy Hadronic Behavior

Again, if the photon behaves like a ρ meson, we have the unique opportunity to study the characteristics of vector-meson-nucleon scattering. In particular, what are the implications of the striking new results on the forward pp elastic cross-section from the ISR[13] for our measurements of $\frac{d\sigma}{dt}\ (\gamma p \to \gamma p)$ near the forward direction ? Also, what will be the relationship between our measurements of $\sigma_{tot}\ (\gamma p)$ and the various new total cross-section results from Serpukhov[14] ?

Validity of Vector Meson Dominance

At NAL, there will no doubt be measurements of

$$\frac{d\sigma}{dt}\ (\gamma p \rightarrow v^o p) \quad v^o = \rho,\ \omega,\ \phi,\ \ldots$$

at high energies. The well-known proportionality between the sum over these vector meson photoproduction cross-sections and the Compton cross-section

$$\frac{d\sigma}{dt}\ (\gamma p \rightarrow \gamma p) = \sum_v \frac{e^2 m_v{}^4}{4\gamma_v{}^2}\ \frac{d\sigma}{dt} \quad (\gamma p \rightarrow v^o p)_{(\text{transversely polarized } v^o)}$$

may or may not be satisfied by today's data[15) - the errors are too large to really tell. At NAL energies, non-diffractive contributions will have died away, and the ratio of photon-vector-meson couplings should be close to that predicted by SU (3). Again, we have high hopes of learning more about the hadronic character of the photon, and hence about the validity of the vector meson dominance picture.

F. More on the Hadronic Character of the Photon

There are aspects of the hadronic interactions of the photon which are clearly not explainable in the vector dominance picture; for example, deep inelastic lepton-nucleon scattering. Therefore all the questions of interest in strong interactions (e.g., do total cross-sections rise with energy, do diffraction peaks shrink, etc.) in fact are doubly interesting for γp interactions because they involve not only the further understanding of hadrons through vector mesons, but also the understanding of the complete nature of the photon coupling to hadrons.

II. $\sigma_{tot}(\gamma A)$

A. Deuterium

Reported differences[16] between σ_{tot} (γp) and σ_{tot} (γn), which imply a sizeable isovector exchange contribution in Compton scattering (from the optical theorem), are expected to disappear at high energies. Will they? Recent data from Serpukhov[14] showing a difference between $\sigma_{tot}(\pi^+p)$ and $\sigma_{tot}(\pi^-p)$ also make possible differences between n and p targets a point of interest.

B. Heavier Nuclei (Be to Pb)

A value of 120 μb for σ_{tot} (γp) corresponds to a mean free path in nuclear matter of ~700 f. This is considerably larger than typical nuclear radii, which are on the order of a few fermi, so that, naïvely, we would expect to find

$$\sigma_{tot}(\gamma A) = A\,\sigma_{tot}(\gamma p).$$

However, the vector-meson-dominance model implies that the photon wave inside the nucleus behaves partly like a hadron (ρ, ω, ϕ, ...) wave. Coherence between photon and vector meson waves inside the nucleus will then produce shadowing as in πA interactions, which display a behavior

$$\sigma_{tot}(\pi A) = A^{0.75}\;\sigma_{tot}(\pi p).$$

We expect σ_{tot} (ρA) to look similar from quark model considerations, and so then should σ_{tot} (γA).[17]

Measurements of $\sigma_{tot}(\gamma A)$ at energies between 3 and 15 GeV indicate that indeed shadowing does occur[16], but by no means with the full strength observed in $\sigma_{tot}(\pi A)$. The best fit appears to be $A^{0.9}$.

This might be explained in several ways, two of which we mention. First it may be that the photon is not entirely a vector meson, or that $\sigma_{tot}(\rho N)$ is in fact much smaller than $\sigma_{tot}(\pi N)$, which would lead to an intermediate shadowing. Second, it may be that the finite vector meson mass causes the shadowing to change with energy, reaching the $A^{0.75}$ dependence only at high energy. Several model calculations[18] using the ρ, ω, ϕ vector mesons make an intermediate shadowing in the 5-15 GeV range plausible. There are then several possibilities:

1) We observe $A^{0.9}$ at all energies above 20 GeV. This would imply that $\sigma_{tot}(\rho N)$ is much smaller than $\sigma_{tot}(\pi N)$ at high energies.

2) We observe $A^{0.75}$ at all energies above 20 GeV. This would imply that the models which depend on the mass of the vector mesons are correct, that the vector mesons involved have a mass in the region of the ρ, ω, and ϕ, and that $\sigma_{tot}(\rho N) \simeq \sigma_{tot}(\pi N)$.

3) We observe A^n, where n is a function of energy between 20 GeV and 200 GeV. This would imply the existence of one or more heavy vector mesons, since in order to get energy dependence above 20 GeV, the mass of the vector meson with which the photon couples must be considerably larger than the ρ, ω, ϕ masses.

III. $\gamma p \rightarrow \gamma$ + Hadrons

The next step, to be run concurrently with σ_{el} (γp), is the measurement of deeply inelastic photon-nucleon scattering. This experiment will in its first exploratory step, use the same basic shower detection techniques.

The most obvious questions to be answered by this experiment are the following:

If the hadronic interactions of the photon are very much like those of the ρ meson, we do not expect any sizeable large-angle photon yield (there is no deeply inelastic meson-nucleon scattering). Will we see a distinctive departure from this picture here ?

Sizeable large-angle yields at high energy have been observed in electron- and muon-scattering, and have been inferred for neutrino-interactions. All these particles are, to the best of our knowledge, pointlike and structureless. Does the photon display any aspects of a behavior so typical of pointlike particles ?

In this sense, inelastic photon-nucleon scattering is intimately related to deeply inelastic lepton-nucleon scattering, a field which has recently proven to offer some of the most promising insights into the hadron structure problem. The "scaling" behavior of such reactions for electrons and muons was observed in inclusive experiments detecting the scattered leptons only; our group is presently involved in an effort to use the distinctive trigger signal of a large-angle, high-energy muon to fire the 2 m streamer chamber at SLAC for a measurement of all charged final-state particles.

In a similar way, we propose in this experiment to first check whether there is indeed a detectable yield of high-energy, large-angle photons - which provide an equally unique trigger. Depending on the yields to be found, we will then check on scaling properties of this cross-section, and use available additional counters to assemble some information on accompanying hadrons.

The concept of this experiment was worked out by Budnitz and Heusch[19] in the 1969 NAL Summer Study, following a model calculation by Bjorken and Paschos[1]. These authors relate inelastic photon scattering to lepton scattering in a parton model: photons scatter incoherently off pointlike virtual partons. To the extent that the impulse approximation approach of Feynman[20] and Bjorken[21] and the perturbative field theoretical approach of Drell, Levy and Yan[22] have been shown to yield parallel predictions, we have a theoretical handle for our expectations from this experiment: in particular, the dependence of the cross-section on the kinematical variables can be interpreted in terms of the properties of the partons participating in the process. Bjorken and Paschos[1] derive an interesting relationship between inelastic photon-nucleon cross-sections:

$$\left.\frac{d^2\sigma}{d\Omega dE'}\right|_{\gamma p} = \frac{\nu^2}{EE'} \left.\frac{d^2\sigma}{d\Omega dE'}\right|_{ep} \frac{\langle Q^4\rangle}{\langle Q^2\rangle}$$

where E, E' are initial and final projectile energies, $\nu = E-E'$. This simple relationship will quickly tell us how seriously we can take the model; and, if taken at face value, it tells us about the mean parton charge $\langle Q\rangle$ - no matter how we realize the partons.

It has recently been pointed out by Brodsky and Roy[23] that the two approaches mentioned above are equivalent, for processes involving two photons, only under very restrictive assumptions: in particular, that the two photons couple at the same instant to one parton line only according to the diagram

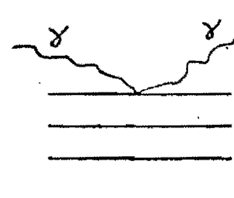

Only if graphs of this type dominate deeply inelastic photon scattering in the kinematical region of interest to our experiment will we expect results interpretable in either framework; conversely, a full set of data may help to decide the relative merits of these two approaches.

While these ideas spur our interest, and the specific model helps to estimate counting rates, we may accept them as nothing beyond an intimation that indeed sizeable amounts of large-angle, high-energy photons may be observed, in excess of what we expect from radiative decays of secondary hadrons.

Suppose we do observe such events: what value will a good measurement have quite apart from the parton model ?

The graph

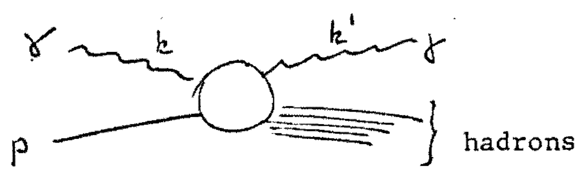

involves two photons with $q^2 = (k - k')^2 > 0$. For one-photon processes, the connection between time-like and space-like behavior has been of considerable interest in the case of

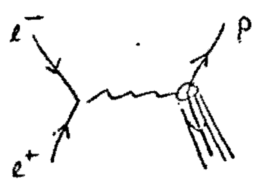

and

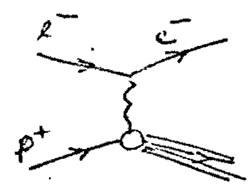

.

Two-current problems have recently aroused much discussion. We may then similarly study the connection between

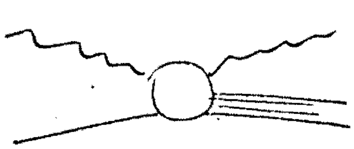

(1)

and

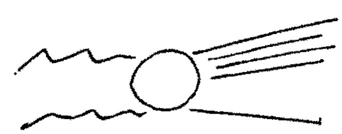

(2)

,

where the latter graph can be measured experimentally in colliding e^+e^- beams as a differential form of the principal part of the Brodsky-Kinoshita graph

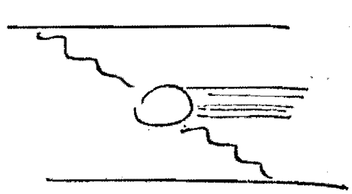

(3)

$\approx$

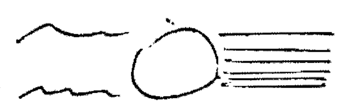

(4)

.

The kinematic regimes of graphs (1) and (4) are, of course, quite different.

Following recent ideas of Mueller[24)] on three-body generalizations of the optical theorem, we can transform graph (1) into

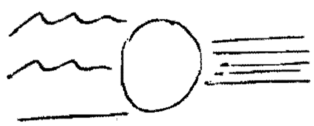

,

(5)

which is proportional to the Imaginary part of

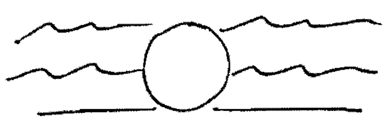

,

(6)

Thus measurement of graph (1) may provide important information on graph (6), a six-point function of considerable theoretical interest.

Electron-Photon Beam

Proton Target

The target for the proton beam should be ~1 interaction length of Be, which from experimental studies is expected to be about 40 cm[25) 26)]. The use of Be minimizes the number of radiation lengths per interaction length, for easily handled metals.

Various schemes for bringing the proton beam onto the Be should be possible, depending on the requirements for e^- flux and π^- elimination. The neutrons that ultimately give us our π^-'s are on the average significantly more energetic than the π^0's which ultimately give us our e^-'s. Thus we expect the background-producing neutrons to have a more forward peaked production distribution than the π^0's and we can cut down the π^-/e^- ratio (and the e^- flux) by bringing the proton beam onto the Be at a small angle with respect to the beam transport system.[27)] The proton targetting system should therefore include several horizontal and vertical bending magnets so that the proton beam direction can be varied.

The optimum length of Be and the optimum proton incidence angle will have to be determined experimentally. Based on calculations, using such models as the thermodynamic model[28)], and using our beam transport system, we feel that we can get a halo-free electron beam of a few x 10^8 electrons at 200 GeV and a photon beam of up to 5×10^5 tagged photons in the upper 35% of the spectrum from this electron beam.

First Conversion Step

The beam produced by the protons passes through a magnetic deflection system which sweeps away, vertically , all charged particles. The remaining neutral beam then impinges on a ½ radiation length radiator.

The photons hitting the radiator produce pairs, with e^-'s accepted by our following beam line. The typical transverse momenta, including multiple scattering, for the pairs are a few MeV/c, so they appear to originate from a small spot in the Be target. The neutrons produce π^-'s which are a potential background source. However the expected transverse momenta of the π^-'s are several hundred MeV/c, so they appear to originate from a much larger spot and can be eliminated selectively at the undispersed foci of the beam. The combined effect of using a Pb radiator and tight slits is expected to reduce the π^-/e^- ratio to $\sim 10^{-3}$.

Beam

A proposed electron-photon beam transport system has been previously sent to NAL, and a copy of that proposal follows. This beam has been designed specifically with the versatility required of a general facility. The beam should be well shielded up through the bending magnet in the third leg. The first two legs, by using variable slits, are capable of delivering various halo-free beams with a minimum of chromatic aberrations. With the last leg of the beam as in our design, we have great flexibility in deciding the final phase space characteristics of the beam at the experimental target. The third leg of the beam should be left readily accessible for change, should future experimenters desire radically different shaped beams.

We propose the construction of the general purpose tagged photon beam, shown in Figure 1. We feel this beam is economical, flexible, has excellent acceptance, and minimizes background problems. This proposal is being submitted to describe the optics of this beam; discussion of such things as the tagging syste experimental target, etc., can be found in the forthcoming U.C.S.C. proposal to measure various photon cross sections.

The beam requires for its construction either 9 or 10 3Q120 quadrupoles (depending on whether it is desired to use one extra quad and less total power), 2 3Q84 quadrupoles, 3 4-2-240 bending magnets, two 5-1.5-120 bending magnets, one 5-1.5-240 bending magnet, and ditching magnets to dump the proton beam. The field strengths for the various beam elements for a 300 GeV electron beam are listed in table 1. The beam has three foci in both planes.

For an early startup on a 200 GeV beam one can use just as easily nine quadrupoles (three in first leg of the beam, four in the second, and two in the third), with the bending magnets and all but three of the quads in the same positions as for the 300 GeV beam.

<u>First leg of Beam</u>

The beam is fully defined in angle by the quads in the first leg of the beam. The acceptance is: (assuming a 3 inch quad aperture)

$|\Theta_x| \leq .60$ mrad. (horizontal plane), $|\Theta y| \leq .95$ mrad. (vertical plane),

and the following two legs of the beam are matched to this acceptance. The bending magnets are purposely spread out to do a good job in eliminating all the off momentum particles created along the beam line.

At the focus the off diagonal beam transport matrix elements are kept small (achieved by starting with a triplet having a unit transport matrix and then moving quads as little as possible from this configuration) which is helpful in keeping the beam small in the following legs. The magnifications are kept at reasonable values at the first focus, to minimize aberrations in the beam, and are chosen so that the overall magnifications at the third focus (experimental target) are not too large. At the first focus the magnifications are -1.68 in the horizontal plane and -.71 in the vertical.

The dispersion at the first focus is 0.30 inches/% $\Delta p/p$ and the beam should be defined to have $\left|\frac{\Delta p}{p}\right| \leq 5$ % which matches the acceptance of the following quad. It would be nice to have a movable horizontal slit at the first focus so that the momentum bite can be varied for different experiments. There should also be a tight vertical slit to absorb π^-'s at the first focus. For $\left|\frac{\Delta p}{p}\right| = 3$ % the maximum size of the beam due to chromatic aberration = .08", which is comparable to the source size. Thus we can have a slit opening whose full aperture ~.2".

The immediate definition of the beam in the first leg, we feel to be a very strong feature of our beam !

Second leg:

This leg has a unit transport matrix and keeps the beam well within the quads - minimizing aberrations. This is very important in the horizontal plane where we wish to put a tight slit to get rid of π^-'s. The first two legs combined have very good properties with respect to aberrations when compared to, for example, such other systems as doublets.

The magnets in this leg are again spread out to most effectively eliminate particles that have been scattered by some beam element, or by the slit. A good feature of this leg is the fact that the dispersion that the beam had at the first focus is quickly decreased as the beam passes through the first quad. This means that we don't need any field lenses and that we don't lose beam at the quads.

The second focus is dispersionless and the slit aperature there should be variable in both the vertical and horizontal planes. This aperture gives us control over π^- backgrounds, momentum acceptance and final beam size - all of which may need to be varied from experiment to experiment.

Third Leg

This is the tagging leg. The magnet near the focus sweeps out slow particles and bends the beam away from any photons which emerge from the slit. This magnet produces a totally negligible dispersion at the third focus. The magnifications at the end of the third leg are -1.2 in the horizontal plane and -2.8 in the vertical. The last two quads in the beam have been taken to be 7 foot quads in order to get a larger aperture in the horizontal plane. This allows us to accept, if we wish, a larger momentum bite because we are now no longer as sensitive to chromatic aberrations. We could, however, use two ten foot quads instead.

The beam has been carefully designed to prevent any particles (which are in the beam in the first two legs) from striking the quads in the last leg. This is very important if we are to avoid both false tags and the pileup of random photons in the shower counters following the target at the third focus.

Some Possible Beams Gotten by Varying Slit Openings

(a) To get rid of the maximum number of pions we could set the horizontal slit at the second focus to a full aperture of about .3 inches. This would give a full width at half maximum for $\frac{\Delta p}{p}$ of 6%. The slit at the first focus would then also be set for approximately this momentum. The vertical slit at the second focus would then have to be set to a small full aperture of only .5 inches to pass this momentum. This would give us a rectangular beam with dimensions: 7 cm x 2½ cm at the tagging target and .85cm x 5cm at the third focus.

(b) If the momentum bite were set at $\left|\frac{\Delta p}{p}\right| \leq 2\%$ at the first focus the final beam size would be reduced to about .75 cm x 3.5 cm, for the same slit setting as above.

(c) For cases where we don't have to worry about pions too much we could open the horizontal slit at the second focus to about .5". By now clamping down the vertical slit at the second focus we could pass a broad momentum ($\left|\frac{\Delta p}{p}\right| \leq$ 4 to 5 %) beam whose final size at the third focus would be about 2. cm x 2 cm.

(d) We mention an additional option which we gain by having a well defined beam at the first focus: If we insert a thin Pb radiator after the first focus we can shift the electron beam energy relative to the pion beam energy and then remove the dispersion of the electron beam in the second leg. This would get rid of most of the pions at the cost of electron flux, at the second focus.

Acknowledgements:

We would like to acknowledge several informative discussions that Dr. Joe Murray of SLAC had with Abe Seiden.

TABLE I -- BEAM ELEMENTS AND FIELD STRENGTHS FOR A 300 GeV/c ELECTRON BEAM

Beam Element	Type	Distance from primary target (ft)	Strength (Quads; kG/1.5 in.) (Bends; kG)
Q1	3Q120	95	-7.8
Q2	3Q120	132	4.744 } Can replace with one quad
Q3	3Q120	143	4.744 }
M1	4-2-240	159	11.0 (0.384°)
Q4	3Q120	241	-6.5166
M2	4-2-240	280	11.0 (0.384°)
FIRST	FOCUS	340	
Q5	3Q120	355	7.4714
M3	5-1.5-120	365	12.0 (0.209°)
Q6	3Q120	414	-7.4714
Q7	3Q120	525	7.4714
M4	4-2-240	540	16.313 (0.569°)
Q8	3Q120	584	-7.4714
M5	5-1.5-240	647	12.5 (0.436°)
SECOND	FOCUS	680	
M6	5-1.5-240	686	14.0 (0.244°)
Q9	3Q120	762	-6.2
Q10	3Q120	774	-6.2
Q11	3Q84	799	7.7
Q12	3Q84	807	7.7
TAGGING	SYSTEM AFTER Q12		
THIRD	FOCUS (TARGET)	960	

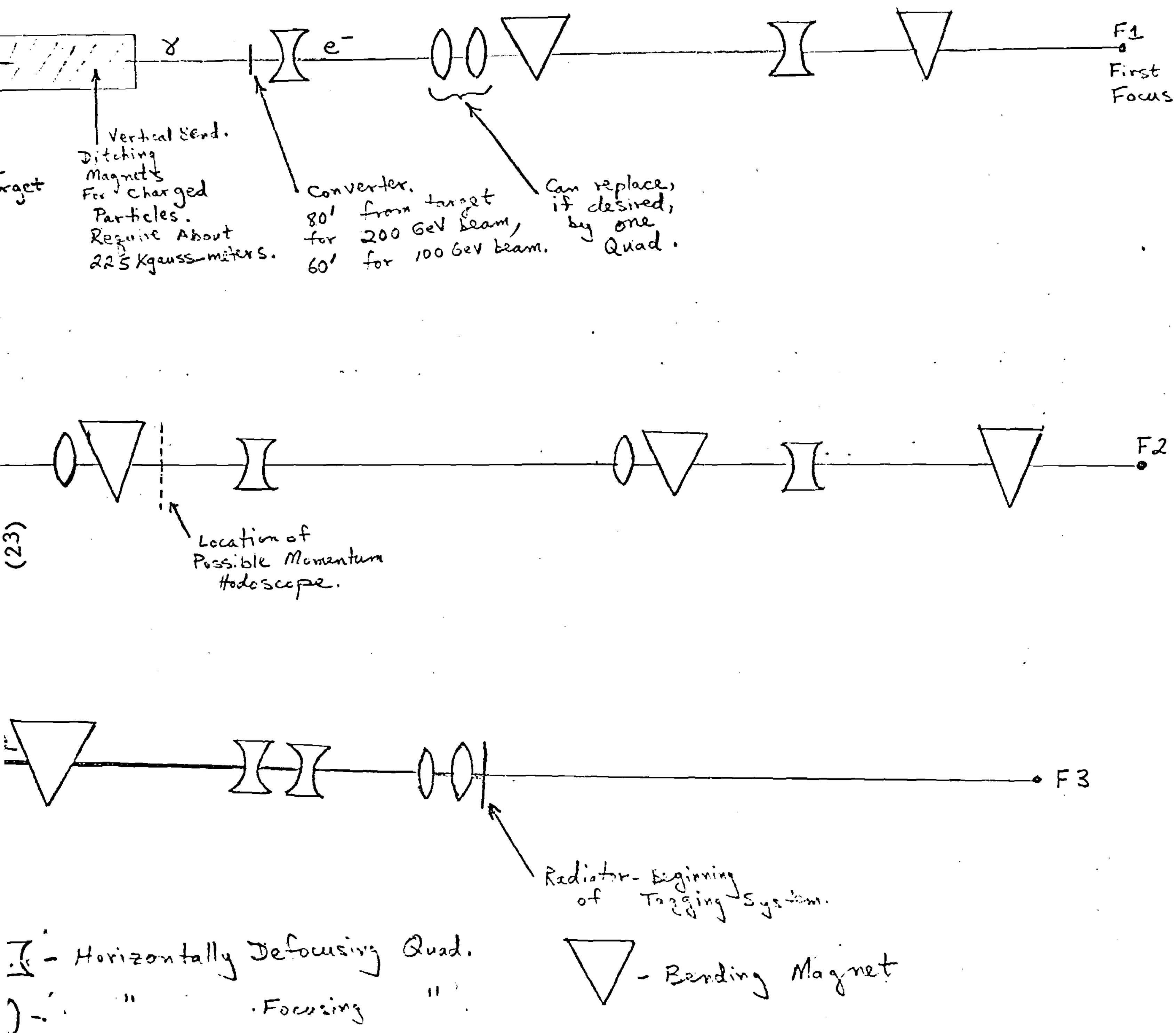

Figure 1.

Proposed Beam

Note: Drawing only Roughly Drawn to Scale.

Photon Tagging System

In the last leg of our beam, the electrons moving down the beam line will traverse a Pb radiator of thickness ≈ 0.01 X^o; about 0.5% will emit a bremsstrahlung quantum of energy > E/2 (E = beam energy). The decelerated electrons will be deflected vertically be a set of bending magnets (cf. Fig. 2) for momentum analysis. They are subsequently recorded by two proportional wire chambers (for accurate momentum definition and vertical position measurement), a scintillator hodoscdpe (for measurement of lateral displacement in the beam, and for fast triggering), and shower counters for electron identification and energy determination. In addition we are including a small scintillator (which can be used as a veto if desired) to monitor possible tridents and the radiation of untagged photons of energy > 50 GeV within several nanoseconds of a tagged photon. We can wherever necessary also put in counters to detect the e^+ in trident production.

We have talked to the director of the CEA who has told us that we may have availabe to us two CEA H magnets, and one CEA C magnet, which in combination bend the highest-energy electrons sufficiently. By appropriate setting of the magnet currents, we can tag any desired fraction of the photon spectrum.

The set of 2 shower counters in the tagging system (lead lucite Cherenkov sandwich counters 15 X^o thick; for details see section on shower counters) measure the electron energy to an accuracy of $\sigma \approx 10\%$ at 1 GeV, $\sigma \approx 2\%$ at 100 GeV. These shower counters perform various important functions: they identify electrons (versus, say, π^- contamination) and help to avoid mistags; they allow a fairly accurate accounting of the energy balance in the experiment: for all final states which are fully detected, the energies including the tagged electron energy must add up to the beam energy. Their resolution is well-matched to these overall requirements.

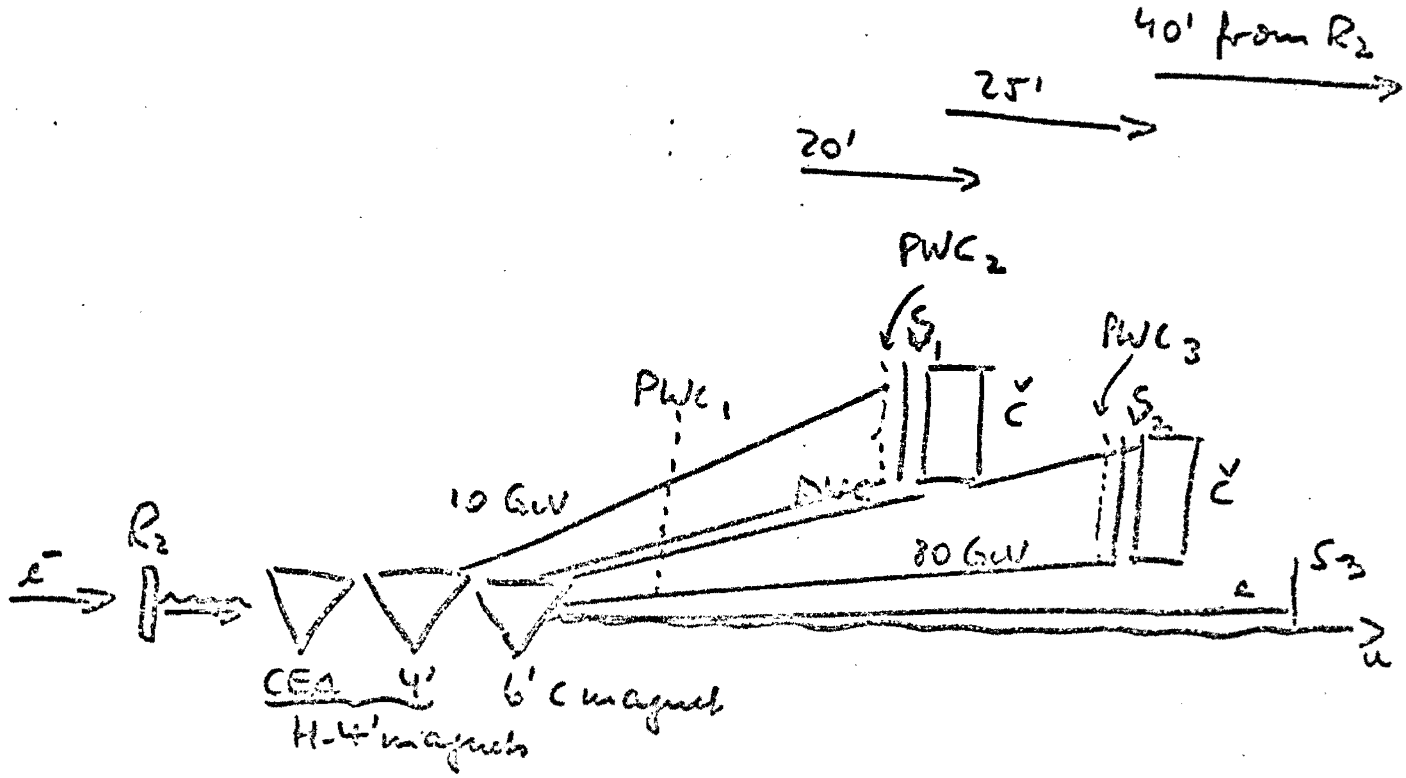

Dimensions: horizontally 4" } for all detectors
vertically 5" – 20" }

S_1 and S_2 are hodoscopes |||||| with 1 cm wide segments

Fig 2: Schematic Drawing of Tagging System.

One advantage of this design lies in the fact that we need only two shower counters: pulse height analysis needs to be performed, and gains have to be kept matched on only 2 phototubes instead of some large array. Note that we will not run into rate problems: we expect $\sim 5 \times 10^5$ tagged photons per pulse; accidental overlays will be negligible.

Measurement of Beam Parameters

In order to analyze our experimental results we need to know, to a reasonable precision, the incoming photon's energy and angle. For example, for elastic scattering we must know the incoming photon angle to a fraction of a milliradian because the cross section is negligible for scattering angles greater than a few milliradians.

Angular Information:

The tagging system has been constructed to yield the maximum information on the position of the e^- which radiated our tagged photon. The scintillation hodoscope tells us the horizontal position of the e^- to about ± .5cm. Using two sets of proportional chambers we get not only the final electron momentum but also its vertical position to ± .5 cm. Since the tagging system also measures vertical position, we remove any constraints on beam size at the tagging radiator -- allowing us to accept as large a momentum bite as we wish without losing spacial information.

The information on position has to be turned into angular information. In the horizontal plane, our final beam size of ~ .85 cm makes this easy. Taking into account correlations in the beam, with a distance of 150' from the Pb to the target, we can measure the horizontal angle to ± .15 mrad. The vertical position at the Pb radiator is known to about ± .5 cm from the proportional chamber measurements. However, the final beam can be large in the vertical plane, so we can only measure the vertical angle if we have vertex information at the target. This limits our Compton scattering measurements to the cases where the recoil proton escapes from the target. Given vertex localization we can also measure the vertical angle to about ± .15 mrad.

Measurement of the Tagged Photon Energy:

Since the electron beam energy has such a wide momentum spread, the tagged photon energy would only be known to ~ ± 5% if no further measurement were made on the beam.

To measure the incoming electron energy we propose to put a momentum hodoscope four feet after the first bending magnet in the second leg of the beam. Because the first quad in this leg of the beam focuses horizontally, the beam size not due to dispersion, at this point is only a little larger than at the first focus. The dispersion at this point is .28 inches per % $\Delta p/p$ and the full size of the beam is 2½ inches in the horizontal plane. Placing the momentum hodoscope early in the beam improves our resolution because the chromatic aberrations are smaller than further downstream.

A spatial measurement of .75 cm at the hodoscope gives us a momentum measurement for an electron, good to ±½ %. By using thin scintillators we can keep the number of electrons which lose this amount of energy, by straggling in the scintillator, to a few per cent. Proportional chambers in the tagging system give the momentum of the decelerated electron with considerable accuracy so that the resolution in tagged photon energy is essentially determined by the momentum hodoscope.

A trigger signal from the counters downstream of the experimental target, and a coincident tagging signal, will cause the momentum hodoscope to be interrogated, with a time resolution of a few nanoseconds. If desired, events with signals in more than one counter of the hodoscope can be vetoed.

An alternative method for measuring the incoming electron energy would be to place a horizontal bending magnet just in front of the tagging radiator. The resultant horizontal displacement of the tagged photon, which would require vertex localization information, would then give us the momentum of the electron it came from.

Detection System: A. General, overall description.

The basic setup of final-state detectors is shown in Fig. 3 :

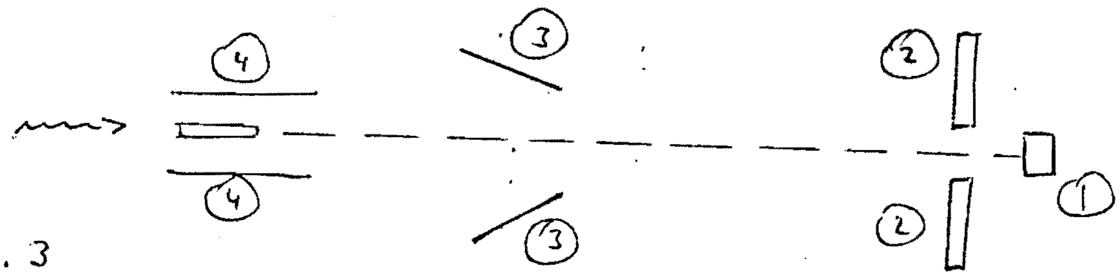

Fig. 3

It consists of the following elements:

(1) forward shower detector/hodoscope
(2) small-angle shower-hadron hodoscope
(3) intermediate angle detector
(4) recoil detector

The individual elements are described in more detail below. The information to be provided by these elements for the experiments is the following:

σ_{tot}: (1) provides shower energy and location for non-interacting γ, or e^+e^- pair generated in the target ;
(2), (3), (4) indicate that no hadron was produced .

σ_{el}: (1) provides shower energy and photon trajectory (together with beam hodoscope, tagging information);
(2), (3) indicate elasticity of the event, while
(4) gives recoil proton angle (for coplanarity test) and, crudely, its energy by range .

σ_{inel}: (1), (2) give shower energy and location, test for possible neighboring showers or hadrons ;
(2), (3), (4) tell crudely about accompanying final-state particles, charged multiplicity, shower or no shower, emission angle.

π^o, η^o, $X^o \rightarrow 2\gamma$, ... (1), (2) give pertinent information on double or triple showers ;
(1), (2), (3), (4) tell crudely about accompanying particles.

The overall strategy is then:

all exp'ts: (1) (or (2)) indicate high-energy shower, define its parameters precisely in conjunction with beam, tagging information ;
(1)...(4) are then strobed for information leading to identification of individual event types.

B. Individual Detectors

General Characteristics of Shower Counters

The measurement of shower parameters (trajectory, energy) becomes basically simpler with rising energy. This is due mostly to the decreasing importance of fluctuations on the shower development as the total number of shower particles (and hence the total track length) increases. At low energies, up to a few GeV, fluctuations of longitudinal spread, location of the shower maximum, and the number of charged shower constituents at any given penetration depth are the principal features that limit good resolution.

At high energies, as considered in this proposal, the number of charged shower constituents becomes large, opening angles are small, fluctuations are relatively unimportant. Longitudinal and lateral dimensions increase only logarithmically with energy, so that counter sizes remain reasonable, and do not limit obtainable resolutions.

The small fluctuations on shower constituents at given depths make discontinuously sampling shower counters -equivalent to continuously integrating devices (like lead glass counters). The large number of charged constituents of $\beta \approx 1$ further makes the light output of a Cherenkov radiator as informative as that of a scintillator.

We therefore propose to use throughout the system lead-lucite sandwiches as originally developed by members of our group[29]: they should furnish excellent, adaptable, and cheap detectors for the photonic final states which are our principal concern.

The localization of points along shower trajectories will be performed by crossed scintillator hodoscopes and proportional wire chambers to be inserted at strategic depths into the shower counters. This ought to be done, for optimum trajectory definition, at depths large enough to ensure a high conversion efficiency for incident photons, and close enough to the shower vertex so as not to allow significant subsequent lateral spread. Such hodoscopes/spectrometer can be built in such a way that the energy loss in the converters gets added to that dissipated in the principal radiators, so that there is no overall loss in energy resolution due to the localization requirements[30].

The energy resolution to be obtained can be confidently expected to be $\sigma \gtrsim 2\%$ at 100 GeV; tests of lead-lucite and lead-scintillator sandwiches show, up to SLAC energies, an energy trend as detailed in fig.4 [31]. Although these curves will not continue to follow the $\sigma / \mu \propto E^{-\frac{1}{2}}$ trend to arbitrarily small widths, the lead-lucite counter is certain to reach the desired precision for 50-100 GeV.

Shower Telescope (1)

This Shower Telescope has to fulfill the following requirements:

- Accept all non(strongly) interacting events - i.e., be of a geometry to contain the beam shadow;

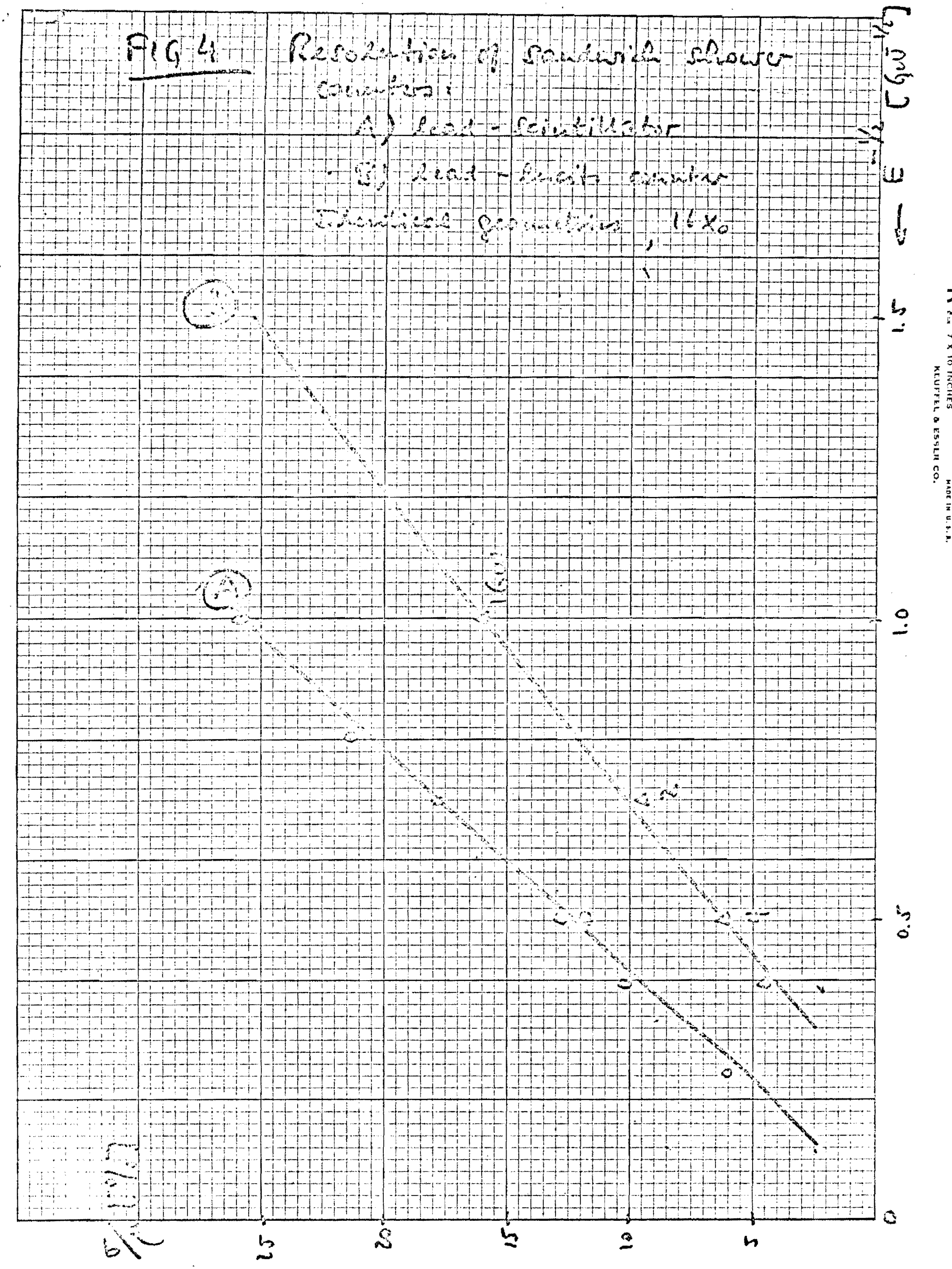

FIG 4 Resolution of sandwich shower counters:
A) lead - scintillator
B) lead - lucite counter
Identical geometries, 16 X0
(A)
(B)
1.5
1.0
0.5
0
25
20
15
10
5

- Recognize showers vs. non-showers, measure shower energies to a few percent;
- Locate one or two points along the shower trajectory to a few mm.
- Tell charged from neutral incoming particles.
- Yield all the above information in the presence of expected overall counting rates of $\lesssim$ several Mc/sec.

Fig. 5 shows schematically the makeup of this telescope. It consists of a veto counter to identify incoming charged particles;

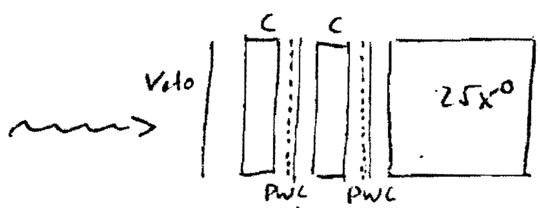

Fig. 5

Two converters for photons (of variable lead thickness inserted between three lucite sheets each) with subsequent scintillator crossed hodoscopes, and finally a lead-lucite samdwich counter of 25 X^o thickness, 25 fingers. The area is 12x15 cm^2; readout from the side. The hodoscopes have 4 mm segments. The distance from the target is ~20 m; this distance is determined by the necessity to (a) distinguish neighboring showers from radiative meson decays, and (b) determine t values for scattered photons with an accuracy commensurate with the definition of the incoming photon direction (~0.2 mrad).

Shower Telescope (2)

The outer shower counter serves these purposes:

- identify all high-energy showers, locate them accurately;
- measure shower energies; reject low-energy showers;
- identify non-showering hadrons.

This counter subtends the region from very small t values out to 30 mrad. The overall counting rate is expected to be small. Fig. 6 shows a schematic design:

Looking downstream:

hole for non-interacting photons, e^+e^- pairs

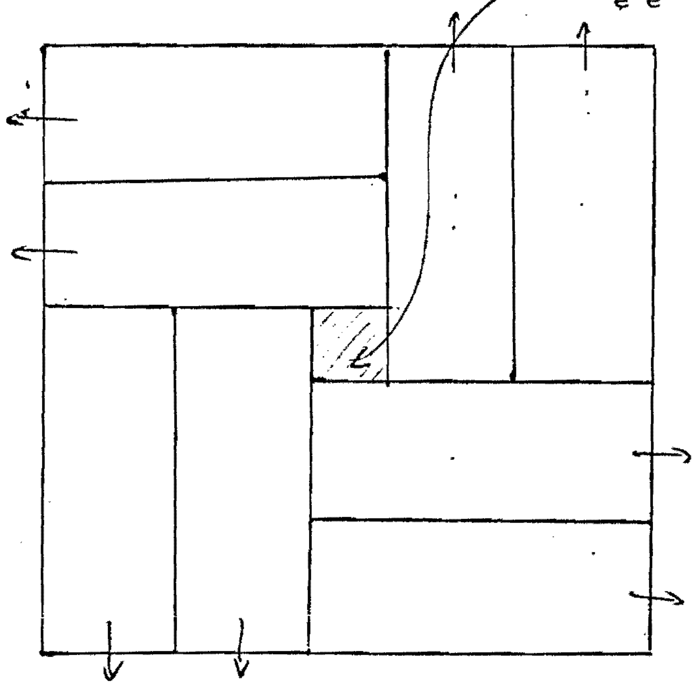

fig. 6

There are eight shower counters of transverse dimensions 46x98 cm^2; the sequence is, for incident particles (Fig. 7)

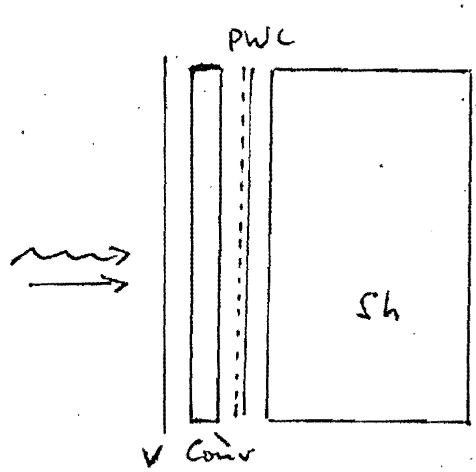

fig. 7

veto counter, converter, proportional chambers, lead lucite counters, there may be a doubling of the converter - PWC system, depending on the outcome of our SLAC tests.

Hadron Counter (3)

This is a system of crude intermediate-angle counters, spanning the laboratory angular range from 30 mr to ~ 45^{0}. There are four counters, scintillators with some absorber material in front (to exclude soft electromagnetic backgrounds from drifting into this large-solid-angle device).

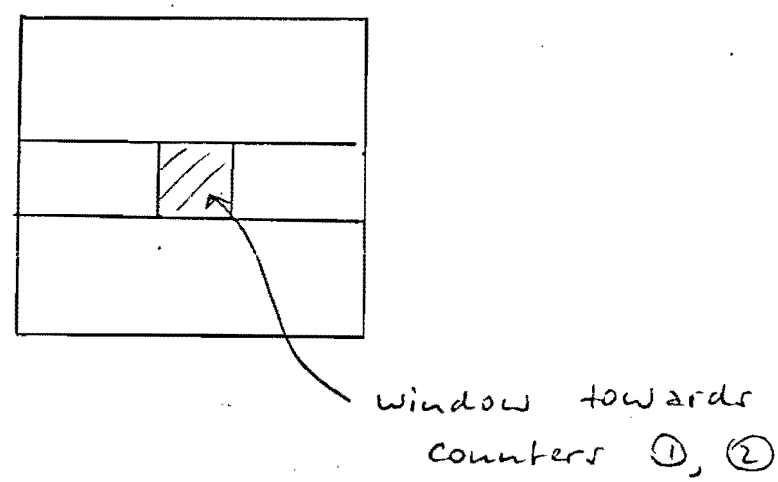

Its function is simply to record intermediate- and large - angle secondaries which do not hit the recoil detector. The precise geometric size will be determined by the geometric location far upstream of shower counter (2).

Recoil Detector (4)

This is a large-solid-angle device surrounding the liquid-hydrogen target. Its function is the accurate determination of the angle of a recoiling nucleon, and a crude measurement of its energy by range. It is designed mainly to meet the requirements of the elastic Compton experiment, where the recoil protons emerge with laboratory angles between 45 and 90°. It is schematically shown in Fig. 8

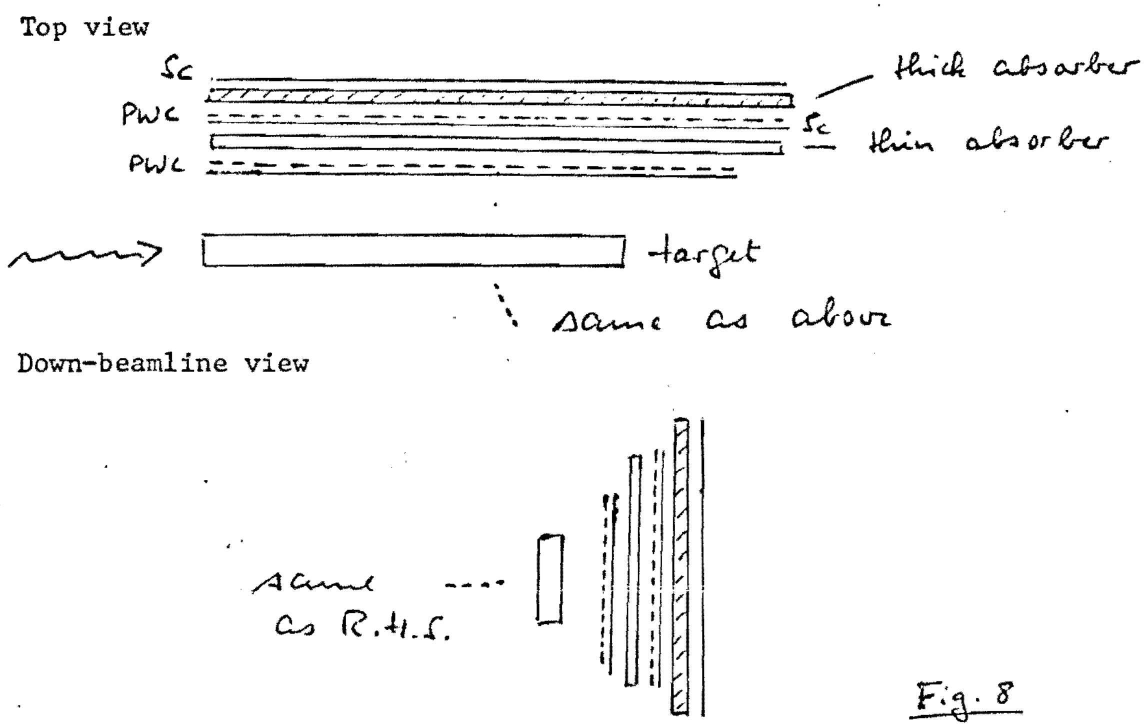

Fig. 8

Two sets of PWC's determine the trajectory of the recoil proton, if it emerges sideways; scintillators give the triggers, the absorbers tell it from backgrounds.

For up- or down-going protons, we demand only a count from a longitudinal scintillator hodoscope. In this view, the target is narrow, so that reasonably accurate complanarity information can be gained.

Note: Counter systems (3) and (4) can be substituted by the large-angle and recoil detection devices designed by the MIT-Canada collaboration, should they be available and appropriately dimensioned.

Rates and Backgrounds

I. Measurement of σ_{tot}

We base our estimates of data-taking rates on a reference value of 100 μb for the hydrogen cross section independent of energy. The A dependence is expected to be between $A^{2/3}$ and A; therefore we take the worst case (from the point of view of rate and background) of $A^{2/3}$ and give the enhancement factors for the case of $\sigma \propto A$. All targets will be 0.1 radiation length; thus the pair production rate is 1 per 10 photons before rejection by our trigger system. Table II shows the rates to be expected in our experiment, with given beam intensities.

The rapid loss of photon flux as the electron energy rises beyond 200 GeV indicates that it is not worthwhile, to go beyond 200 GeV for a complete set of high-Z elements. We therefore propose to do a complete set of elements at 40 GeV and 200 GeV, and a complete energy dependence for H and Aℓ, from 40 GeV to 300 GeV. We will obtain statistical accuracies of better than 1%, for each element at 40 and 200 GeV; for H and Aℓ we will obtain better than 1% for each bin of 10% $\Delta E/E_\gamma$ from 25 to 300 GeV (except for Aℓ at 300 GeV where we obtained 3% errors). The running time required for data-taking (exclusive of check-out time) is 60 hours (for σ_{tot}). Table III lists the running time required for each part of the experiment.

Backgrounds

1) Pair production in the target: These will be vetoed by the shower counter (1) Very asymmetric pairs may have a low-energy electron emerging at larger angle due to multiple scattering in the target. In such cases, an off-line check will reveal that the counter (1) received all the γ energy, so the event will be thrown out.

2) False tags: The rate of false tags can easily be kept below 1% of good tags. A possible background can come from accidental coincidences between the tag and a count in the hadron detector. At a very conservative 3000 false tags/sec, 10 nsec resolution, we must keep the singles rate of the hadron detector less than 300 times the true hadron rate to maintain 1% accuracy.

3) Non-interacting photons: A large shower in counter (1) with no hadron signal will veto the event. Rejection is similar to the pair production case.

II. Elastic Compton Scattering on Hydrogen

Measurements at lower energies[32] have given a cross-section approximately fit by

$$\frac{d\sigma}{dt} = (0.7\ \mu b/\mathrm{GeV}^2)\ e^{8t}$$

The trigger for $\gamma p \rightarrow \gamma p$ must be a coincidence between a proton in the recoil detector and a high energy photon in the final shower counter. Protons with momentum less than 300 MeV/c do not get out of the hydrogen target; we may then estimate the total visible elastic Compton cross section as

$$\sigma = 0.50 \int_{(0.1\ \mathrm{GeV}^2)}^{\infty} \frac{d\sigma}{dt}\, dt = 20\ \mathrm{nb},$$

where 0.50 is a (conservative) detection efficiency for the recoil proton.

We propose to make a 3% measurement of the slope and intercept of the forward differential cross section. This measurement will require 2000 events, which for a photon flux of 3 x 10^5/pulse and 0.1 r.l (1 meter) of liquid hydrogen will require 100 hours of data-taking (see Table III).

Background Rejection Methods:

Coplanarity : The measurement of the scattered photon direction, the initial photon direction and the proton azimuth in the recoil detector gives a strong co-planarity constraint. For example, less than 0.1% of events of the type $\gamma p \rightarrow \gamma N^*$, which were Monte Carlo generated for $M_{N^*} < 3$ GeV, gave an event satisfying coplanarity to the accuracy we expect to achieve.[33]

Transverse momentum balance: The magnitude of the transverse momentum of the outgoing photon must be equal to the transverse momentum of the recoil proton if the event is elastic. Since t_{pp} is a more useful variable we will express the constraint by indicating how well we measure t in two independent ways:

1) $t \approx (k\theta_{\gamma\gamma})^2$. The resolution for this determination is determined mainly by the resolution in $\theta_{\gamma\gamma}$, the angle between the incoming and outgoing photons. The incoming photon is known to ± 0.2 mr. The outgoing photon covers 25 meters and can be measured to ± 3 mm in the shower array. Thus $\Delta\theta_{\gamma\gamma} \approx \pm\, 0.25$ mr. We write

$$\Delta t \approx 2k\sqrt{t}\;\Delta\theta_{\gamma\gamma} \approx \frac{k}{2000}\sqrt{t}$$

At a typical t of 0.25 GeV^2 we find $\Delta t = 0.05\ GeV^2$ at $k = 200$ GeV

2) $t \approx p^2_{1ab}$ of the proton. Here Δt at 0.25 GeV^2 will be approximately 0.03 GeV^2 (independent of k).

Proton angle: There is a correspondence, for elastic events, between the momentum transfer to the proton, t, and the proton angle with respect to the incoming photon. We can express this relation by another equation for t;

$$t \cong 4\, m_p^2 \cot^2\theta_{\gamma p} \quad \text{for } E_\gamma \gg Mp$$

Thus $\Delta t \cong 8m_p^2\ (\pi/2 - \theta)\ \Delta\theta$

and, at $t = 0.25\ GeV^2$ we find $\Delta t = 0.01\ GeV^2$ for $\Delta\theta = 5$ mr, a reasonable value to achieve. Below $t = 0.25\ GeV^2$ this determination of t deteriorates rapidly due to multiple scattering in the target.

Energy Conservation: The difference between the initial and final photon energies in elastic scattering is less than 1% for the t range of interest. We can measure the initial and final energies to a few percent.

The four methods above, taken together, simply represent the four constraints in a reaction where the momentum of all particles are known. A proper four-constraint fit will in fact be used to extract all possible information from our measurements.

Background sources are radiative meson decays and inelastic Compton events; both are expected to be negligible when the above criteria are applied.

III. Inelastic Compton Scattering

For the purpose of estimating a counting rate, we follow Bjorken and Paschos.[1] Their cross section expression is:

$$\frac{d^2\sigma}{dtd\nu} \doteq \frac{\alpha^2}{4k^2\sin^4\theta/2}\left[\nu W_2\ (t,\ \nu)\right]\frac{\nu}{kk'}\ \frac{<Q^4>}{<Q^2>}$$

where $<Q^2>$ is the mean square charge on a pointlike constituent. The corresponding form for inelastic electron scattering is:

$$\frac{d^2\sigma_{ep}}{dtd\nu} \doteq \frac{\alpha^2}{4k^2\sin^4\theta/2}\left[\nu W_2\ (t,\ \nu)\right]\ 1/\nu$$

It has been found from ep scattering that $\nu W_2 \approx 1/3$. Taking a simple quark model one finds that $<Q^4>/<Q^2> \sim 1/3$. Therefore we can express

$$\frac{d^2\sigma}{dtd\nu} \approx \frac{63\ \text{nb}}{(\text{GeV}/c)^2\text{GeV}}\left[\frac{(k-\nu)\ \nu}{k^3t^2}\right]$$

Integrating over ν from zero to $\nu_{max} = 0.5\ k$

$$\frac{d\sigma}{dt} \approx \frac{6.3\ \text{nb}/(\text{GeV}/c)^2}{t^2} \qquad (t \text{ in GeV}^2)$$

The integral of this function above $t = 1\ \text{GeV}^2$ gives 6 nb which is 1/3 of the visible elastic Compton scattering in our experiment. In other words the two processes might be comparable in magnitude.

On the other hand, if one calculates the diagram:

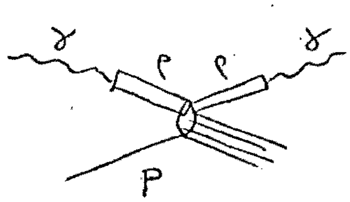

One expects a much steeper exponential-like fall with t, which would predict negligible cross section above $t = 1(\text{GeV}/c)^2$. With 100 hours of running we will certainly be able to determine whether the cross sections at large momentum transfers are anything like the point-constituent model predicts, since we would expect on the order of 600 events.

Backgrounds

The presence of π^0's produced in γp interactions gives a large number of photons in the forward direction. Their energy is usually much lower than the energy of the incoming photon, thus they prevent us from looking at large ν events. The question is how large a ν can we reach before π^0 contamination swamps our measurements, taking into account that we can distinguish two photons from a π^0 in most cases in our final shower array.

We have calculated the expected photon background from inclusive π^0 production[28] and from $\omega \to \pi^0\gamma$ for reasonable values of the ω production cross section. The results are shown in Figure 9, where we have assumed that 90% of the time we have rejected the background event because it has multiple photons. We see that as t increases we can with confidence check the model at higher energy loss of the photon.

FIGURE 9

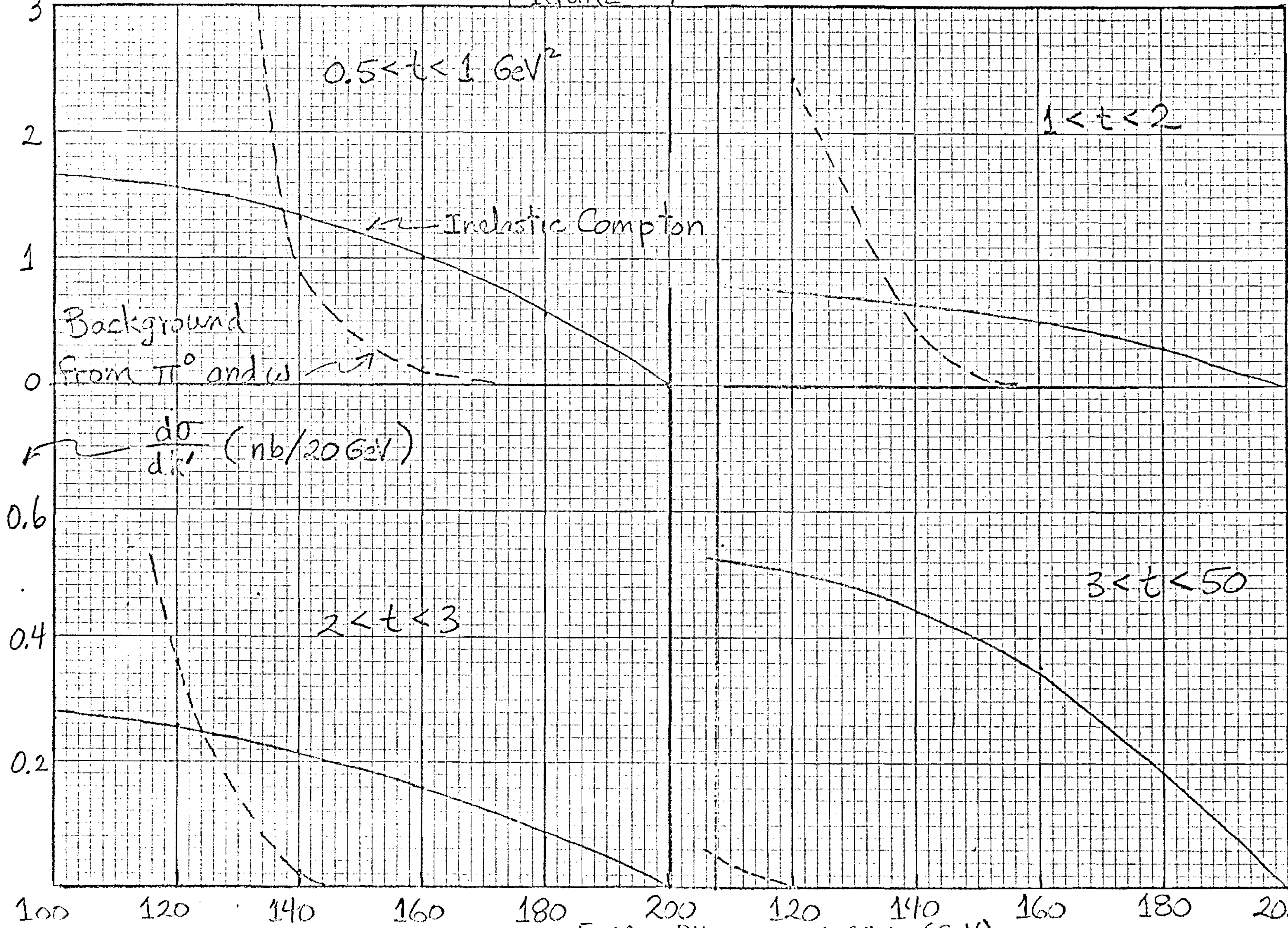
0.5 < t < 1 GeV²
1 < t < 2
2 < t < 3
3 < t < 50
Inelastic Compton
Background from π° and ω
dσ/dk′ (nb/20 GeV)
3
2
1
0
0.6
0.4
0.2
100
120
140
160
180
200
120
140
160
180
200

Running Time

Actual data-taking requires 160 hours, however the σ_{total} experiment requires 30 different energy-target combinations, and check-out requirements (including target-empty runs) are substantial. Therefore we feel that the total running time for the experiment will be 300 hours of prime time. Some set-up time at low intensity will be very helpful to the efficiency of the experiment.

Table II Rates for σ_{tot}

	$\left(\frac{\text{Rate } (A^{2/3})}{\text{Hydrogen Rate}}\right)$	Rate/photon	pairs per Hadronic event	Rate per Hour (200 GeV or less)	Rate Hour^{-1} (300 GeV)	Enhancement in Hadronic rate if $\sigma \propto A$ instead of $A^{2/3}$.
H	1	1/2500	250	$1.2\text{x}10^5$	4000	1
D	1.6	1/1700	170	$1.8\text{x}10^5$	6000	1.26
Be	0.53	1/5000	500	$6\text{x}10^4$	2000	2.1
C	0.32	1/8300	830	$3.6\text{x}10^4$	1200	2.3
Al	0.14	1/18000	1800	$1.7\text{x}10^4$	600	3.0
Cu	0.05	1/47000	4700	6400	200	4.0
Sn	0.03	1/83000	8300	3600	120	4.9
Pb	0.019	1/130000	13000	2300	70	5.9

Table III Running time (hours)

Element / Energy (GeV)	H	D	Be	C	Al	Cu	Sn	Pb
180-300	10				10			
120-200	100*	0.06	0.17	0.3	3	1.6	3	4.5
84-140	0.5				3			
60-100	0.5				3			
42-70	0.5				3			
30-50	0.5				3			
24-40	0.5	0.06	0.17	0.3	3	1.6	3	4.5

Total Running time: 160 hours

*) The 100 hour run is mainly for Compton Scattering (both elastic and inelastic)

Equipment and Personnel

Beam: We expect to assist in all stages of building and testing the beam.

Tagging System: The same applies. We will also build and test the tagging shower counters. The tagging magnets will probably be available from the CEA.

Targets: We request a 1 m liquid H_2 and D_2 target from NAL.

Detection equipment: We will design, build and test all shower detection equipment prototypes. We may seek financial assistance for the large-area shower counters. We will attempt to share as much equipment as possible with other groups, notably MIT - Canada. In particular, we hope we will be able to arrange the use of proportional wire chambers + readout equipment from the Canadian group.

Electronics: We hope to use largely NAL standard fast fast logic.

Computing: We will need a small computer for on-line data analysis, and for equipment check as well as kinematics determination. If available from NAL, we will apply for use. Otherwise we will procure our own.

Manpower

5 PhD physicists and 3 graduate students will be involved in this program. Of the experienced people 2 will be permanently located in Batavia to help on all aspects of the facility, as soon as the project is approved.

REFERENCES

1) J. D. Bjorken and E. Paschos, PR 185, 1975 (1969).

2) C.A. Heusch, UCRL 16830, Vol. III, 156 (1967)
NAL Summer Study Vol. II, 156 (1968)
NAL Summer Study Vol. I, 163 and 167 (1969)
W.T. Toner, NAL Summer Study Vol.II, 125 (1968)
R. Diebold and L.N. Hand, NAL Summer Study I, 149 (1969)

3) C. A. Heusch, ref. (2) and NAL Summer Study Vol. I, 203 (1969)
UCRL 16830, Vol. III, 182 (1967)
C.A. Heusch and R. J. Budnitz, ref. 19

4) beams: μ beam for SLAC: S. Flatté and A. Seiden, LRL Group A Internal Note (1971)
A. Seiden, UCSC Internal Note #2 (1971)
$e(-\gamma)$ beams for NAL : cf. Ref. (2) above
A. Seiden, UCSC Internal Note #4 (1971)
shower detection: C.A. Heusch and C.Y. Prescott, IEEE Trans.Nucl.Sc.: 12, 213, (1965)

5) M. Gell-Mann, M.L. Goldberger, and W. Thirring, PR 95, 1612 (1954)

6) S.L. Adler & R.F. Dashen, Current Algebras, W.J. Benjamin, N.Y. (1968)

7) M. J. Creutz, S.D. Drell, and E. Paschos, PR 166, 1768 (1968)

8) V. D. Mur, JETP 44, 2173 (1963); 45, 1051 (1963).

9) M. Damashek and F.J. Gilman, PR D1, 1319 (1970).

10) H. Cheng and T. T. Wu, PRL 24, 1456 (1970), and previous papers listed there.

11) H. Cheng and T.T. Wu, DESY preprint 71/36 (1971)

12) See, e.g., a graph on p. 14 of R.E. Taylor, Proceeding of the International Conference on Expectations for Particle Reactions at the New Accelerators, (1970)

13) M. Holder et al., CERN preprint (1971)
U. Amaldi et al., CERN preprint (1971)

14) J. V. Allaby, private communication (1971)

15) D. W. G. S. Leith, SLAC - PUB 679 (1969)

16) D. Caldwell et al., PRL 23, 1256 (1969)
H. Meyer et al., Phys. Lett. 33B, 189 (1970)
V. Heynen et al., DESY 71/5 (1971)

17) L. Stodolsky, PRL 18, 135 (1967)

18) B. Margolis and C. L. Tang, Nucl. Phys. B10, 329 (1969)
K. Gottfried and D. R. Yennie, PR 182, 1995 (1969)
M. Nauenberg, PRL 22, 556 (1969)

S. J. Brodsky and J. Pumplin, PR 182, 1794 (1969)

19) R. J. Budnitz and C. A. Heusch, NAL Summer Study 1969, Vol. 4, 171

20) R. P. Feynman, unpublished

21) J. D. Bjorken, PR 179, 1547 (1969)

22) S. D. Drell, D. J. Levy and T. M. Yan, PR 187, 2159 (1969)

23) S. J. Brodsky and P. Roy, PR D3, 2914 (1971)

24) A. H. Mueller, PR D2, 2963 (1970)

25) W. Galbraith et al., BNL 11598

26) J. Cox et al., Nucl. Instr. and Methods 69, 77 (1969)

27) C. A. Heusch, NAL Summer Study Vol. 1, 203 (1969)

28) M. Awschalom and A. VanGinneken, NAL Internal Report FN-216 (1970)
M. Awschalom and T. White, NAL Internal Report FN-191 (1969)

29) C. A. Heusch and C. Y. Prescott, CTSL - 41 (1964)

30) C. A. Heusch et al., Proc. Dubna Instrumentation Conference (1970)

31) C. A. Heusch and C. Y. Prescott, unpublished

32) A. M. Boyarski et al., SLAC - PUB - 872 (1971)

33) W. Ross, private communication (1971)

Addendum to NAL Proposal 152

D.E. Dorfan, S.M. Flatté, C.A. Heusch,
G. Luxton, C. del Papa, A. Seiden.

We wish to add a few remarks to our photon physics proposal: first, to bring out several distinguishing points of our project, which we believe need to be stressed; and second, to elaborate slightly on its overall potential. This is done in the hope of facilitating an early decision on approval of this experiment.

1.) The sequence of activities under this proposal - quite apart from work on the beam and on the tagging facility - is designed to take advantage of every stage of the beam development:

The first electron and photon beams, no matter how weak, can be utilized for work on the detection of electromagnetic showers and measurement of their parameters: longitudinal and lateral spread, charged multiplicities at given depths, etc. This set of measurements is of considerable intrinsic value, quite apart from its serviceability for this and other experiments.

Utilizing the data thus obtained, photon trajectory and energy reconstruction can be studied and optimized; this is vital for all subsequent work, and well might benefit many other NAL projects.

A relatively broad-band beam can be used for the measurement of σ_{tot} (γp) and σ_{tot} (γA). We do not expect σ_{tot} to change rapidly over 5-10 GeV at 100-200 GeV: a beam without momentum hodoscope will do. In addition, our detection method is <u>not</u> dependent on one particular beam profile or phase space at the target - there are no stringent optics requirements.

σ_{el} (γp) can likewise be measured without a momentum hodoscope:

the precise knowledge of the photon trajectory is much more important than that of its energy. A $\frac{\Delta k}{k}$ of several % would be perfectly acceptable.

The same is true for an inclusive measurement of γ, π^o, η^o, ... final states. Only for a determination of missing masses would we need better incoming energy definition: this is not foreseen for the first generation of this experiment.

In short, we can do much of our experiment while the beam is by no means optimal, and are relatively insensitive to its phase space at the target location.

2.) The photon spectrum emanating from the tagging radiator is a bremsstrahlung spectrum, slightly modified by the finite width of the impinging electron beam. Should the design parameters of the NAL machine not be met at some point, this program can still proceed with relatively minor modifications: the electron spectrum generated by the chain $p+A \rightarrow \pi^o \rightarrow \gamma\gamma \rightarrow e^-$ is so steep (the upper end of the spectrum is being depleted at every step along this line) that lacking intensity can be made up by moving slightly down in energy. Typically, a factor of 10 loss in intensity at the upper end of the spectrum (say, at 300 GeV) can be made up by moving down to 240 GeV. There is little loss in intrinsic interest caused by this shift in energies, although we would clearly prefer the higher one. Hence, we are not very sensitive to whether or not the NAL proton synchrotron will soon achieve its design intensity.

3.) The approach we have taken builds up an experiment which, on the one hand, will detect final states that are certain to be well-measurable, and are of unquestioned physics urgency; and, on the other hand, it will be highly sensitive to totally new and therefore more speculative measurements. Here, again the physics motivation is strong, but the mechanisms of production and decay are largely unknown, so that we cannot give data collection rates except by the use of restrictive assumptions.

In the first category, we will measure showers in the forward direction with considerable precision: this will lead to precise data on the total hadronic photon cross-section; and, together with information from the recoil detector, to data on Compton scattering.

In the second category, our overall sensitivity to showers emerging even at large angles, plus the hadron detectors, put us into a position to measure the total yields ("inclusive cross-sections") for γ, $e\pm$, π^{o}, and other particles decaying radiatively or into electron modes. This comprises inclusive π^{o}, η^{o}, ω^{o}, ... cross-sections, "inelastic Compton" scattering, pair production through heavy photon intermediate states; it also means we are sensitive to certain decay modes of such putative objects as Dirac monopoles, heavy leptons, and intermediate bosons.

4.) Measurement of π^{o}, η^{o}, ... yields.

We expect to resolve shower energies to an accuracy of $\lesssim 2\%$ at high energies, shower locations (close to the vertex) to $\lesssim 3$-5 mm. Fig. 1 gives a few typical opening-angle distributions for the 2γ decays of π^{o}, η^{o}, and X^{o} mesons. It illustrates the fact that, at 30 m distance from the target, we should be able to distinguish the separate showers from all these decays; and gives a feeling for the confidence level with which we can tell, say, π^{o}'s and η^{o}'s of given energy apart.

In the presence of several neutral mesons in an average final state, the question will arise whether photon showers will not lead to conclusion (i.e., which 2 showers come from the same decaying meson).

We have convinced ourselves that opening-angle distributions at given energy will make the necessary corrections bearable.

Measurements of inclusive π^o (and η^o) production are of considerable interest because they constitute our best chance to test the fragmentation rules relatively clearly in high-energy photoproduction. Feynman[1] conjectured that, in high-energy collisions of two hadrons A and B of momentum p_A and $p_B = -p_A$, the probability of finding a final-state particle C with longitudinal momentum $p_{z,C} = xp_A$ for the upper end of its x spectrum will be given by

$$f\ (x) = (1-x)^{1-2\alpha\ (t)} \qquad \text{for } x \lesssim 1.$$

Here, $\alpha(t)$ refers to the leading trajectory that can carry away the quantum numbers necessary to change particle A into particle C (excluding the Pomeranchuk trajectory).

This result, which was recently derived also by de Tar et al.[2], means that, in photoproduction, where the ρ and ω trajectories ($\alpha_{\rho,\omega}$ $(t=o) \approx 0.5$) dominate, f(x) will be a flat distribution at its upper end

$$f(x) = (1 - x)^o \rightarrow \text{flat} \quad \text{for } x \lesssim 1,\ t \rightarrow o$$

For charged π inclusive photoproduction, this behavior may well be masked by the abundant occurrence of $\rho^o \rightarrow \pi^+\pi^-$ decays: $\pi\pm$ distributions from ρ^o decay will be characterized, simply from decay kinematics, by a distribution function

$$f'(x) \propto (1 - x) \quad \text{for } x_c \lesssim 1\ ,$$

i.e., there will be a linear decrease at the upper end of the spectrum. Note that we have not made any assumptions about the function f (x) resulting from the (mostly diffractive) production of the ρ^o mesons. The decay channel, which is not taken into account in the inclusive models, may therefore determine the x_π distribution for charged mesons.

For π^o, there is no ρ decay, but $\omega^o \to \pi^+\pi^-\pi^o$ might lead to some confusion (lessened by the 3-body decay); also, the small branching ratio $\omega^o \to \pi^o\gamma$ may give some high-energy π^o's. We are studying the possible implications of these admixtures, but expect them to be small (both production and decay channel are suppressed relative to the ρ case).

The study of $\gamma p \to \eta^o + \ldots$ will obviously be free from any such admixture; and, although experimentally harder, it will therefore be of considerable separate interest.

5.) "Odd" objects decaying into showering particles:

Our setup is highly sensitive to all showers in the final state. Mono-energetic photons may well couple to, or pair-create, "odd" or hitherto unobserved objects which decay characteristically into final states containing showers: we will thus be able to identify them depending on their production cross-section.

In particular, assume an object of mass m decaying into 2 photons or electrons of energies k_1, k_2. Thus the invariant mass of the decaying object, for small opening angles θ between the two decay photons,

$$m^2 = 2\, k_1\, k_2\, (1 - \cos\theta) \approx k_1 k_2\, \theta^2$$

will be resolved according to

$$\frac{\Delta m}{m} = \frac{\Delta k_1}{2k_1} + \frac{\Delta k_2}{2k_2} + \frac{\Delta\,\theta}{\theta} \quad .$$

The first two terms on the RHS are of order 1% each as long as the decays are not all too far from symmetric; the third depends strongly on θ : for a 100 GeV π^o decaying symmetrically and being detected 30 m away, $\frac{\Delta\Theta}{\Theta} \simeq 4\%$, $\frac{\Delta m}{m}$ will typically be of order 3% - 10%.

Such an object might be a heavy photon, $\gamma' \to e^+e^-$; in the form suggested by Lee and Wick[3] as a negative-metric pole in the photon propagator, it changes the customary

$$\frac{1}{q^2} \text{ into } \frac{1}{q^2} - \frac{1}{q^2-k^2} = \frac{1}{q^2} \quad \frac{m^2}{m^2-q^2} .$$

In this form, the modified photon propagator has a convergence factor which alleviates the divergences that have plagued QED calculations of radiative corrections. Lee and Wick showed that if this "heavy photon" has finite width, then the modified propagator can exist without violating unitarity or macrocausality. Does such a particle exist? From e^+e^- storage ring data and the muon (g -2) experiment we can set a lower limit on its mass of [4].

$$M_{\gamma'} > 5 \text{ GeV}/c^2.$$

The scaling behavior of inelastic electron scattering may imply[5] that the traditional photon propagator cannot be modified by a massive pole below 8 GeV/c^2.

Clearly, our tagged photon experiment of incoming energy 100-200 GeV could see a wide-angle pair up to considerably higher masses. Note that, if it occurs due to a diagram like

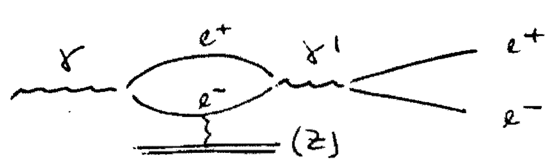

its detection off higher - Z nuclei would be enhanced: it should show up during the σ_{tot} (γA) measurements.

Another ghost in our particle gallery is the Dirac monopole. It might be pair-created and subsequently annihilate into a splash of photons[6]: our apparatus would be ideally suited for its detection and identification. Again, the combination of trajectory and energy measurement of the showers would make confusion with multiple π^o events very unlikely. There are more objects that we may be able to identify from characteristic decay modes : the intermediate boson W and heavy leptons may be pair-produced by the incident tagged photons and then detected through the leptonic final states

$$\gamma \rightarrow W^+W^- \rightarrow e^+e^- + \text{neutrinos}$$

$$\rightarrow e\,\mu + \text{neutrinos}$$

$$\gamma \rightarrow \ell^+\ell^- \rightarrow \text{(similar decays with more neutrinos)}$$

While other experiments may produce these particles more plentifully[7], pair creation from a photon of known energy gives a powerful kinematic constraint,and our final-state detection system puts us into an excellent position to measure showers (and penetrating minimum-ionizing particles) for an accurate determination of characteristic transverse momentum distributions.

Conclusion

We conclude that

a) the experiment outlined in NAL proposal 152 is well suited to the photon beam development at NAL by utilizing its various stages for a natural sequence of experimentation, starting from shower physics and leading up to its full potential as a detector for photon scattering into a number of final states.

b) The experiment contains parts (σ_{tot}, σ_{el}) which clearly will lead to good results at a high confidence level.

c) Through pioneering use of good multi-shower recognition patterns over a large area, we collect, as a byproduct, data on "inclusive" γ, π^o, η^o, ... photoproduction. Such information is not otherwise available and is of clear theoretical interest.

d) The experiment has considerable potential to look for a number of novel objects in a unique way; and while it might be risky to motivate a major experiment by such vague notions, this potential clearly adds an element of speculation and excitement which we would not want to miss.

References

1) R.P. Feynman, in: High Energy Collisions, ed. C.N. Yang, Gordon & Breach, New York (1969)

2.) C.E. de Tar _et al_. PRL _26_, 675 (1971)

3.) T.D. Lee and G.C. Wick, Nucl. Phys. _39_, 209 (1969)

4.) S.J. Brodsky, Proc.Daresbury Conference (1969)

5.) M. Nauenberg, private communication (1971)

6.) M.A. Ruderman and D. Zwanziger, PRL _22_, 146 (1969)

7.) several NAL experiments are looking for such particles produced from proton, muon, or neutrino beams; at the ISR, from pp collisions. For photoproduction from an intense untagged photon beam, see W. Lee _et al_., NAL proposal 87 (1971).

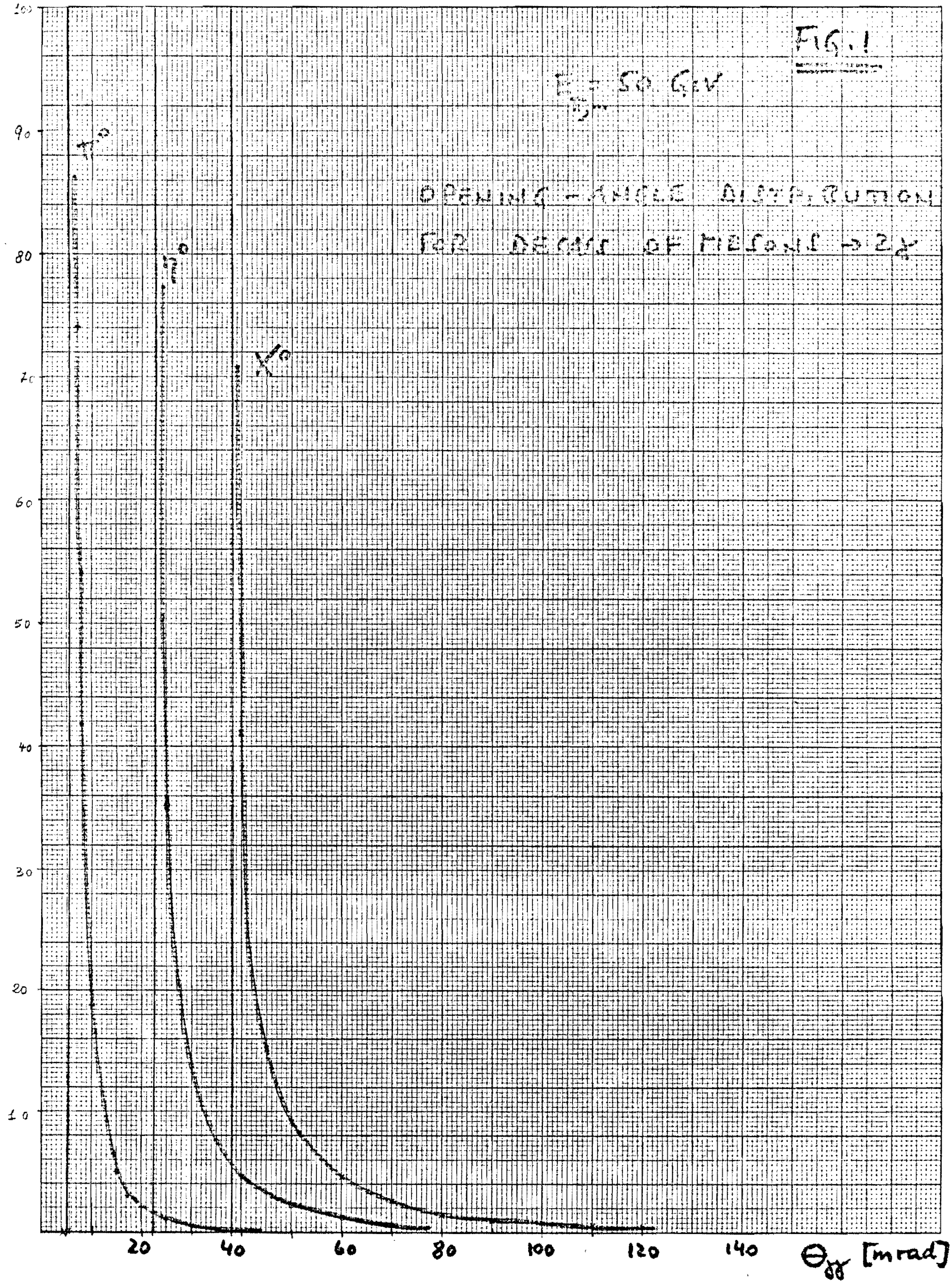

K+E 10 X 10 TO THE CENTIMETER 46 1510
18 X 25 CM. MADE IN U.S.A.
KEUFFEL & ESSER CO.

U.C.S.C. 72/011
June 23, 1972

Addendum II
to
NAL Proposal 152

D.E. Dorfan, S.M. Flatté, C.A. Heusch, G. Luxton,
C. del Papa, and A. Seiden

Division of Natural Sciences, University of California
Santa Cruz, California 95060

Abstract

We propose to perform an early experiment on the processes

$$\gamma p \rightarrow \gamma p \qquad \text{(elastic Compton effect)}$$
$$\rightarrow \gamma + \text{hadrons} \quad \text{(inelastic Compton effect)}$$

in the NAL electron-photon facility. We will use a very simple detection system of shower counters and recoil telescopes, with no magnets. We present counting rates, running time estimates and errors on relevant measured quantities, assuming three possible sets of beam parameters.

In particular, we show that even with very conservative requirements on beam intensities and energy, ~350 hours of running time open up an entirely new regime for Compton scattering: the elastic forward peak and its slope can be measured with good accuracy from 20 to 60 or 100 GeV, depending on the intensity of 200 GeV proton beam; inelastic Compton scattering may show up unambiguously for the first time. Together with the already approved measurement of the total hadronic cross-section $\sigma_{tot}(\gamma p)$, these data will provide vital new information on photon-hadron coupling at very high energies.

Introduction

This addendum updates NAL Proposal 152. After successful initial operation of the National Accelerator Laboratory Proton Synchrotron at energies up to 200 GeV, and after a decision has been reached to install a tagged photon facility which will meet the requirements of this experiment, we address ourselves to the following questions:

1. What are minimum energy and intensity requirements on the primary proton beam for a meaningful experiment on high-energy Compton scattering?

2. What counting rates are accessible? What is the accuracy of determination of relevant parameters?

3. How can we optimize detection efficiency and accuracy, given different sets of intensity and energy parameters?

We discuss mainly the elastic Compton scattering process. Inelastic events will be observed if the cross-section is comparable to the one predicted by the model of Bjorken and Paschos[(2)]. Background events will contain much valuable information on radiative final states, as mentioned in Proposal 152 and Addendum I. However, these do not add to either apparatus design or running time requirements.

Beam Parameter Requirements

We have convinced ourselves that we can perform meaningful measurements of elastic Compton scattering between 20 and 60 GeV with a 200 GeV proton beam at an intensity of 10^{12} per pulse. These measurements will be extended up to 100 GeV for a 200 GeV proton beam of intensity 10^{13} per pulse, and to 200 GeV if the same intensity can be obtained at 400 GeV proton energy.

In the following, we address ourselves to performing elastic and inelastic Compton scattering with a beam of 200 GeV protons, 10^{12} per pulse, and 10^3 pulses per hour. We further suppose that the construction of the tagged photon beam is optimized for a 400 GeV proton beam. This results in a relative loss of intensity by a factor of four since the angular acceptance of the electron beam is determined by its geometry, whereas the electron yield is determined by the acceptance in transverse momentum.[(3)]

There are two methods whereby we plan to regain the lost intensity. First, instead of using the bulk of the running time with an electron beam of 40% of the proton beam energy, for part of the run we will drop the energy to 20% of the proton beam energy, thereby gaining a factor of ~5.[(4)] Second, we increase the thickness of the tagging radiator, from 1% to 3% of a radiation length.

Increasing the thickness of the radiator does not seriously affect the elastic Compton measurement, which has highly overconstrained kinematics; it will increase the systematic error in the inelastic Compton scattering experiment. To reduce the effect of double bremsstrahlung in the tagging radiator, inelastic events that are accompanied by a large shower in the forward shower detector (which subtends an angle of ± 2 mr at the target) will be rejected. Corrections for subtracting good events will be made, based on an extrapolation of the data. This correction is small, since there will be only ~3% significant double bremsstrahlung.

In Table I we give running time and event number estimates, under three different assumptions about the primary proton beam. In Figure 1 we give the statistical errors expected from measurements of the logarithmic slope of the elastic differential cross-section. Also shown in Figure 1 are the corresponding SLAC[1] data.

Counting rates, errors.

For the minimal beam parameters (200 GeV, 10^{12}p/pulse), we will do the elastic and inelastic Compton scattering experiments with an electron beam of 40 GeV/c momentum for 150 hours, and with an electron beam of 65 GeV/c momentum for 200 hours. For the run at the lower momentum, we use a lead radiator of .03 radiation lengths, for the higher momentum, we use a lead radiator of .05 radiation lengths thickness. In this way, we gain useful elastic Compton scattering data over the range 20 - 62 GeV/c. We make ten separate determinations of the slope of the elastic peak over eight distinct energy intervals. The width of the energy intervals is ± 1.8 GeV for the 40 GeV/c run, ± 2.9 GeV for the run at 65 GeV/c.

Assuming $d\sigma/dt = 0.6\ e^{7t}$ μb/(GeV/c), and assuming a conservative efficiency of 80% for detecting the recoil proton for $.05 < -t < .10$ $(\mathrm{GeV/c})^2$, and 90% for protons in the range $.10 < -t < .6(\mathrm{GeV/c})^2$, we expect to obtain 3,900 elastic events with the 40 GeV/c beam and 3,800 elastic events with the 65 GeV/c beam. With these assumptions, the data are plotted, with statistical errors indicated in Figure 2, for the two extreme energy intervals of the 40 GeV/c run. For each of the ten energy intervals, the slope can be measured to a statistical accuracy of about ± 5%; we will be able to detect an energy dependence that is somewhat smaller than this.

When comparing the quoted errors (statistical only) with those of the SLAC data, note that the SLAC errors are largely systematic and result from a subtraction procedure of π^o's and other backgrounds. Our system is sufficiently overconstrained (we resolve both photons from π^o's, detect all recoil protons) to make subtractions insignificant.

To illustrate the accuracy of these measurements, we mention the precision with which we will determine the slope and intercept of an effective Regge trajectory for forward photon-proton scattering. Using

$$d\sigma/dt = \beta(t)\ s^{\,2\alpha(t)-2}$$

$$\mathcal{L} = \ln d\sigma/dt = (2\alpha(t)-2)\ \ln s + \ln\beta(t)$$

$$d\mathcal{L}/dt = 2\alpha'(t)\ \ln s + \beta'(t)/\beta(t),$$

we measure $d\mathcal{L}/dt$, the logarithmic slope of $d\sigma/dt$, as a function of s. This allows us to extract the slope of the trajectory, $\alpha'(t)$ to an accuracy of ± 0.15/GeV^2. We also learn something about $\beta(t)$ by measuring $\beta'(t)/\beta(t)$ to ± 8%. By extrapolating our data to $t = 0$, we determine the trajectory intercept $\alpha(0)$ to ± 0.02. In addition, we will test the consistency of our data with extrapolations of fits to existing data based on the sum of several Regge poles.

Simultaneously with these measurements, we will detect any deeply inelastic scattering that is present to the extent predicted by the Bjorken-Paschos model[5] (2). In Proposal 152, we showed that, assuming observation of all deeply inelastic scattered photons with $|t|>1$ GeV/c^2 and $\nu < .5k$ (where k = energy of the incident photon) we will observe a cross-section of 6.3 nb. This corresponds to 475 events in 150 hours with a 3% radiator at 40 GeV/c. If we observe only those events with $\nu < .3k$, we obtain 200 events in 150 hours. <u>This is a signal that cannot be missed</u>.

To observe this small cross-section, we are naturally concerned about backgrounds. We showed in Proposal 152, however, that for an experiment using a 200 GeV photon beam, we can readily separate deeply inelastic scattered photons from π^o and ω^o decay photons. A Monte Carlo calculation was performed for this purpose, which took into consideration the thermodynamic model for inclusive π^o production as well as diffractive production of ω's. Now the inclusive production of π^o's in the thermodynamic model at high energies depends, apart from an overall normalization factor proportional to $\sqrt{E_{c.m.s.}}$,[(6)] only on the transverse momentum and the fraction of the incident photon energy carried off by the π^o's. This means that the background from inclusive π^o production depends only on t and ν/k[(7)] and is independent of the energy except for the overall normalization factor. Thus the calculations of background given in Proposal 152 may be scaled down to the 40 GeV/c beam merely by reducing the normalization of the background by a factor of 1.64 (the average of $(200/E)^{1/4}$ for a bremsstrahlung beam). This is done in Figure 3. The corresponding factor for the 65 GeV beam is 1.46. At the energies discussed here, we have to consider a source of background that was not included in Figure 3: the "exclusive" process $\gamma p \to \pi^o p$. From data[(8)] at lower energy, we may approximately parametrize the $d\sigma/dt$ for this reaction for $-t > .5(\mathrm{GeV/c})^2$ as $(.6e^{6t}$ +

$.15e^{2t}$) $(15/E)^2$ $\mu b/(GeV/c)^2$, where E is the laboratory energy in GeV. Averaging this over a bremsstrahlung spectrum from 20 to 38 GeV/c and integration over t from $-0.8(GeV/c)^2$ to $-\infty$, we obtain[9]

$$\frac{\int_{20}^{38} dE/E \int_{-1}^{\infty} dt\, d\sigma/dt}{\int_{20}^{38} dE/E} = 4.7 \text{ nb}.$$

With a conservatively estimated rejection rate of 90% due to the observation of both photons from π^o decay, we expect a background of ~35 events. This is reduced to ~14 events at 65 GeV, due to the $1/E^2$ dependence of the cross-section for $\gamma p \rightarrow \pi^o p$.

We achieve the rates quoted due to the use of thicker radiators. These have the systematic effect of increasing the uncertainty with which ν is known. It is therefore important that we discard events in which a significant double bremsstrahlung process has occurred.

A thin radiator is particularly important if the incorrect tag rate must be kept very low, e.g., for a careful measurement of the energy dependence of the total cross-section using a transmission method. With a 5% radiator, a recoil electron with energy (after straggling corrections) of 10% of the beam energy will be accompanied by a photon of ~90% of the beam energy only 88%[5] of the time. The remaining 12% are false tags, or at least are accompanied by tagged photons with substantially incorrect energy. We monitor false tags by rejecting any event with a large shower in the central shower detector. This reduces the contamination due to double bremsstrahlung in both elastic and inelastic Compton scattering to much less than 1%.

Errors in the determination of t, the momentum transfer to the proton, are discussed below, in conjunction with the proton detector. They are small compared to our statistical undertainties.

Detection Apparatus

There are only minor revisions to the apparatus outlined in NAL Proposal 152. For a schematic summary, see Figure 5. The principal elements are a small central shower spectrometer for high rates; a large bank of shower counters surrounding the central detector; hadron counters for intermediate angles; and a recoil detector at angles between 60^{o} and 90^{o}.

The shower detectors measure the location of the shower vertex to $\leq$ 3 mm, the shower energy to $\leq$ 2%. Decays of π^{o}, ω^{o} mesons into photons will be resolved from simple showers up to the highest energies. This makes our project the first Compton experiment which resolves the π^{o} background specifically, thus greatly reducing the systematic errors. The distance between hydrogen target and shower detector is directly proportional to the incident beam energy.

With the accepted beam design[4], we have changed the target configuration to a cylinder of 2.5 cm diameter, 1 m long. This geometry permits a full 2π range for azimuthal detection - an improvement by a factor of ~3 over Proposal 152.

The recoil detector measures proton trajectories with a system of magnetostrictive spark chambers (which may be changed to proportional chambers); pulse-height analysis of dE/dx scintillation counters help to identify and measure the energy of the slow protons.

With three chambers, and a 6" spacing between pairs of chambers and a 1 mm wire spacing, we measure the proton angle to within ± 2.5 mrad. This is especially important for larger values of t for which there is an appreciable probability of obtaining incorrect energy information from the scintillators. For $-t > 0.2(\mathrm{GeV}/c)^2$, we can use the angle measurement to determine the invariant momentum transfer to better than ± 10%; this fractional resolution improves considerably with increasing $-t$. For the smaller values of $-t$, we will identify the proton by requiring a pulse height that corresponds to an energy deposit greater than about twice that of a minimum ionizing particle in a thin counter, and then measure its energy by the pulse heights from several scintillators. The estimated resolution in momentum transfer from this method, including the effect of multiple scattering in target and target walls, is given in Figure 4. An absorber and another counter complete the system.

With this system, the detection efficiency for recoil protons with kinetic energies ≳ 25 MeV is close to 100%.

References and Footnotes

(1) A. A.M. Boyarski et al, Phys. Rev. Letters 26, 1600 (1971).

B. R.L. Anderson et al, Phys. Rev. Letters 25, 1218 (1970).

(2) J. D. Bjorken and E. Paschos, Phys. Rev. 185, 1975 (1969).

(3) This assumes that the transverse momentum distribution is flat up to ~300 MeV/c. This is true to within 20% in the thermodynamic model of Hagedorn and Ranft for secondary particles from 200 GeV collisions that have energies ≥ 100 GeV (M. Awschalom and T. White, NAL FN-191) and these are the particles that are effective in ultimately producing e^- beam particles.

(4) We have scaled the results of "Design of a Tagged Photon-Electron Beam Facility for NAL", C. Halliwell, P. Biggs, W. Busza, M. Chen, T. Nash, F. Murphy, G. Luxton and J. D. Prentice, Nucl. Instr. and Methods, in press (1972)(NAL FN-241). This scaling is approximately valid in the thermodynamic model of R. Hagedorn and J. Ranft (M. Awschalom and A. Van Ginneken, NAL FN-216, and M. Awschalom and T. White, NAL FN-191).

(5) This result is computed from formulas taken from:
Y. Tsai and V. Whitis, Phys. Rev. 149, 1248 (1966),
and L. Mo and Y. Tsai, Rev. Mod. Phys. 41, 205 (1969).

(6) R. Hagedorn and J. Ranft, Suppl. Nuovo Cimento 6, 169 (1968).

(7) These are approximately the same values of t and ν/k as for the photon because of the exponential energy dependence of the π^o spectrum: a photon that fools us for a given value of ν and t

almost always comes from a π^o with approximately the same energy as the observed photon. To retain almost all the energy of the parent π^o, the photon must travel in essentially the same direction as the π^o, and thus have the same t.

(8) The data (and some fits) are reported by Bjorn Wiik in the Proceedings of the 1971 International Symposium on Electron and Photon Interaction at High Energies, p. 164.

(9) We integrate down to $-0.8(\mathrm{GeV}/c)^2$ since in the "exclusive" case there is a non-negligible probability that a photon that fools us has an energy (and angle) quite different from the energy of the parent π^o. Thus the $|t|$ to the photon may be larger than the $|t|$ to the π^o.

Figure Captions

Figure 1 Typical data with statistical errors for the slope of the diffraction peak. Data based on three possible assumptions on beam parameters are displaced from each other to avoid confusion. The expected value for a flat pomeron is ~7 GeV^{-2} at all energies. The different notations for the data refer to the different runs in Table I.

Figure 2 Typical data with statistical errors for the elastic Compton measurement with the 40 GeV/c electron beam. The data are given for the two extreme energy bins.

Figure 3 Deep inelastic Compton scattering cross-section in the model of Bjorken and Paschos[2] as a function of ν and t. The dashed curves represent the background from diffractive ω^o and inclusive π^o production calculated according to the model of Hagedorn and Ranft[6]. The cross-section per interacting beam particle for $\gamma p \to \pi^o$ + anything is taken to be the same as that for $pp \to \pi^+$ + anything. This background is assumed to be suppressed by a factor of 10 by our detection apparatus.

Figure 4 Resolution in t expected from the various methods:

(A) From measurement of the recoil proton angle;

(B) From measurement of the recoil proton energy;

(C) From the measurement of the recoil photon angle (for a 50 GeV photon with the geometry for a 65 GeV e^- beam).

Figure 5 Sketch of the detection apparatus.

Table I. Event Numbers for Various Proton Beams*

	e^- Beam Energy	e^-'s/Pulse	γ Energy	Running Time (Hours)	Number of Elastic Compton ($\|t\| > .05$)	Number of Deep Inelastic Compton ($\nu<0.3k\ \|t\|>1$ GeV^2)
10^{13} protons/pulse at 200 GeV (10^3 pulse/hr.)	40 GeV	7×10^6	20-38 GeV	150	4,000	200
	65 GeV	3×10^6	33-62 GeV	200**	3,900	200
10^{13} protons/pulse at 200 GeV (10^3 pulse/hr.)	40 GeV	7×10^7	20-38 GeV	50	13,300	670
	65 GeV	3×10^7	33-62 GeV	100	11,600	580
	100 GeV	5×10^5	50-95 GeV	200	4,000	200
10^{13} protons/pulse at 400 GeV (450 pulse/hr.)	90 GeV	2.4×10^8	45-85 GeV	50	21,100	1,060
	140 GeV	9.4×10^7	70-133 GeV	100	16,300	820
	200 GeV	2×10^7	100-190 GeV	200	7,200	360

* We have assumed that the secondary electron beam line is optimized for yields from 400 GeV protons, and that our tagging radiator is 3% of a radiation length.

** To increase our rate without using too much running time, we will use a 5% radiator for this run.

$d\sigma/dt = Ae^{Bt}$. Determination of B from the Region $0.05 < -t < 0.6$ GeV^2

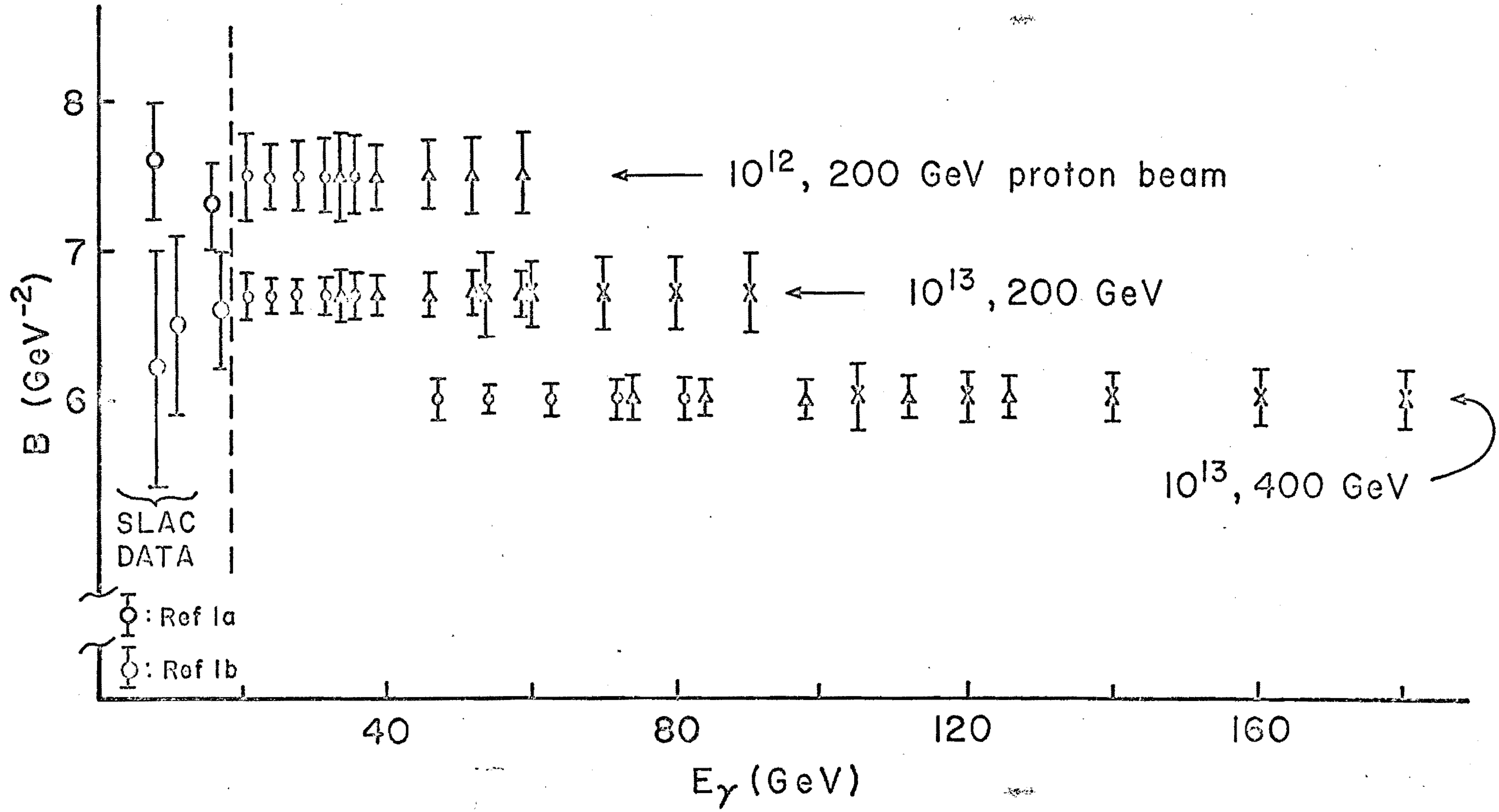

FIGURE I

FIG. 2. Elastic Compton Scattering

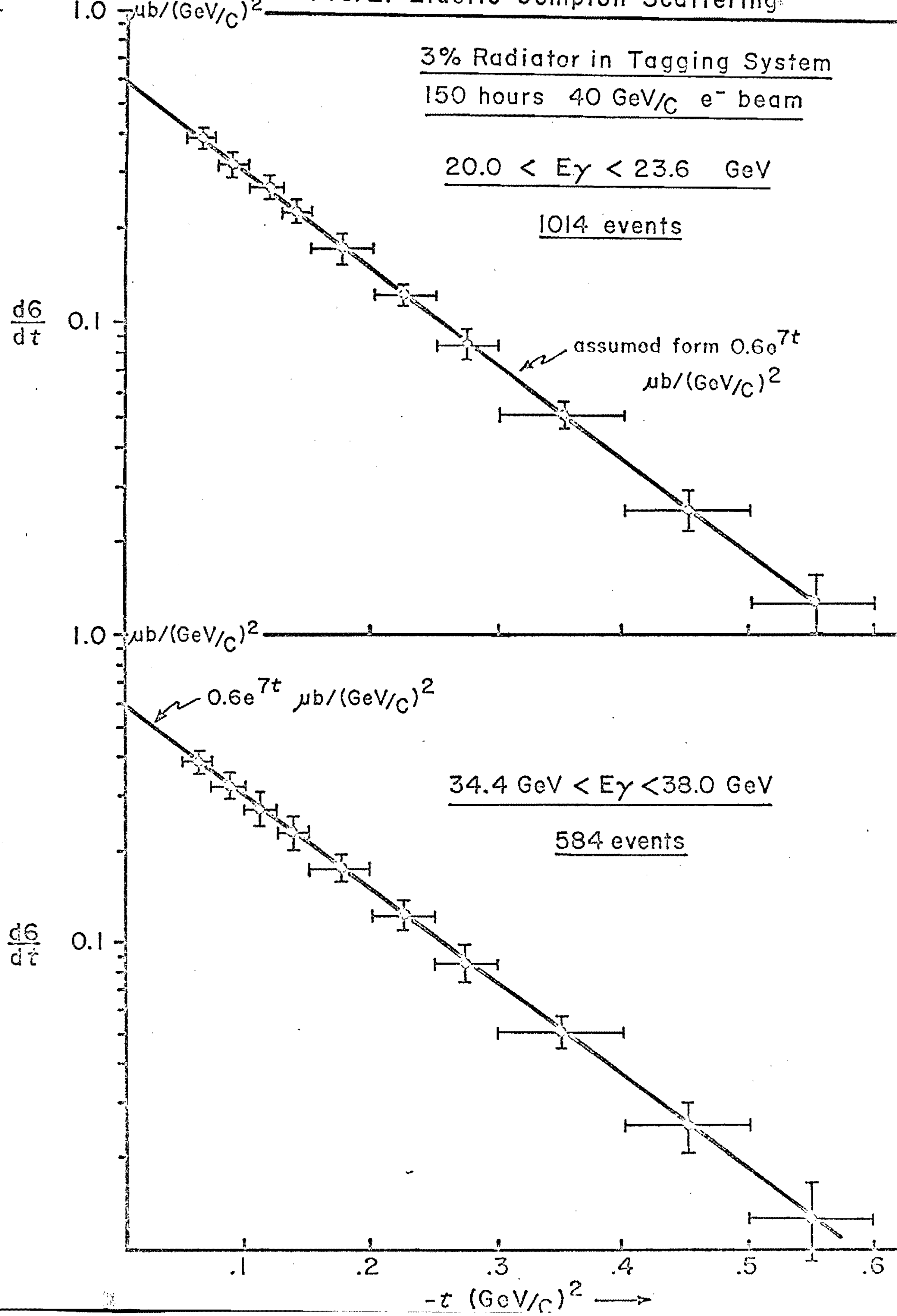

FIG. 3. Inelastic Compton Scattering with 40 GeV/c Electron Beam

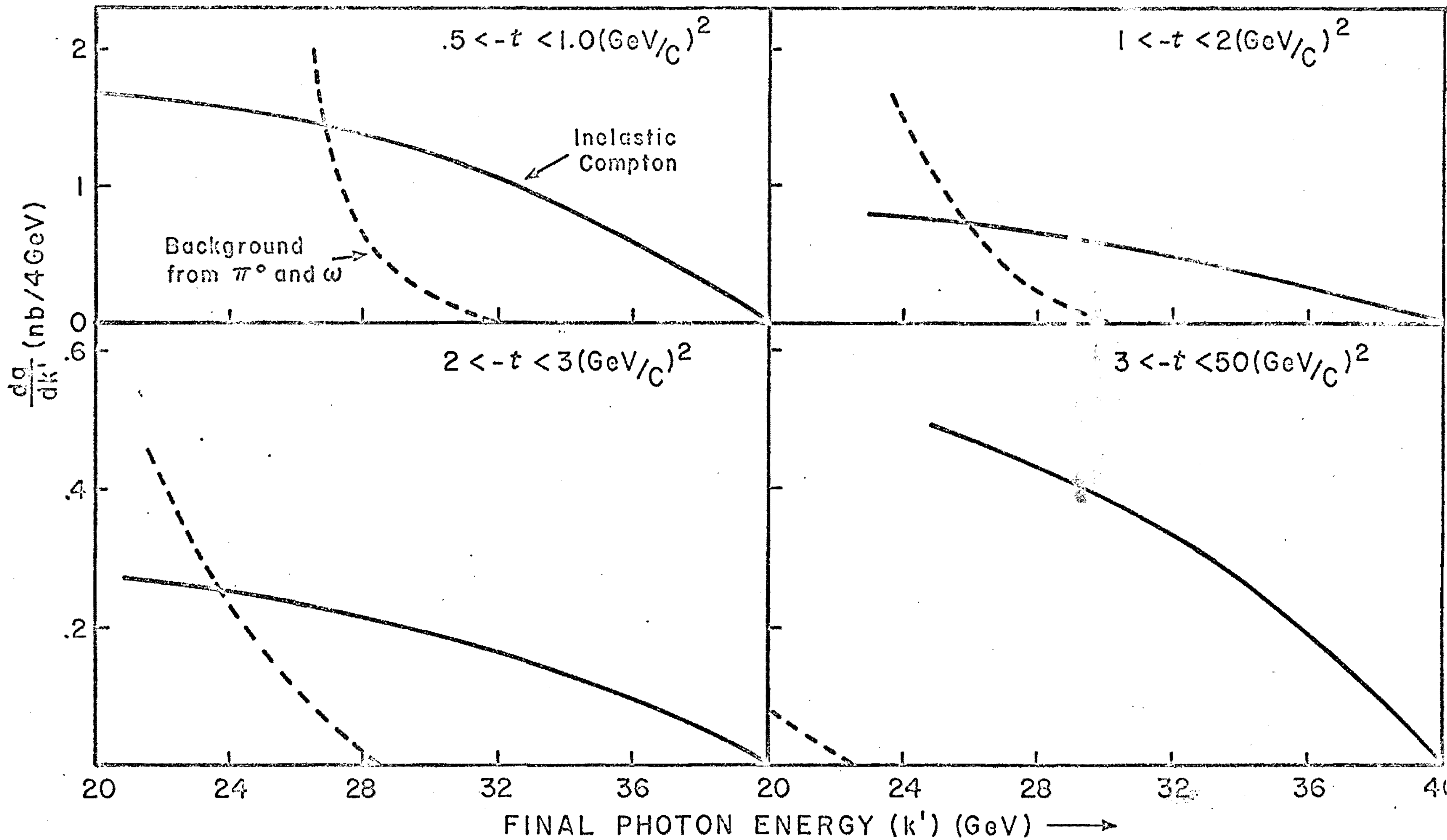

FIG. 4. Elastic Compton Scattering: Estimated Resolution in t

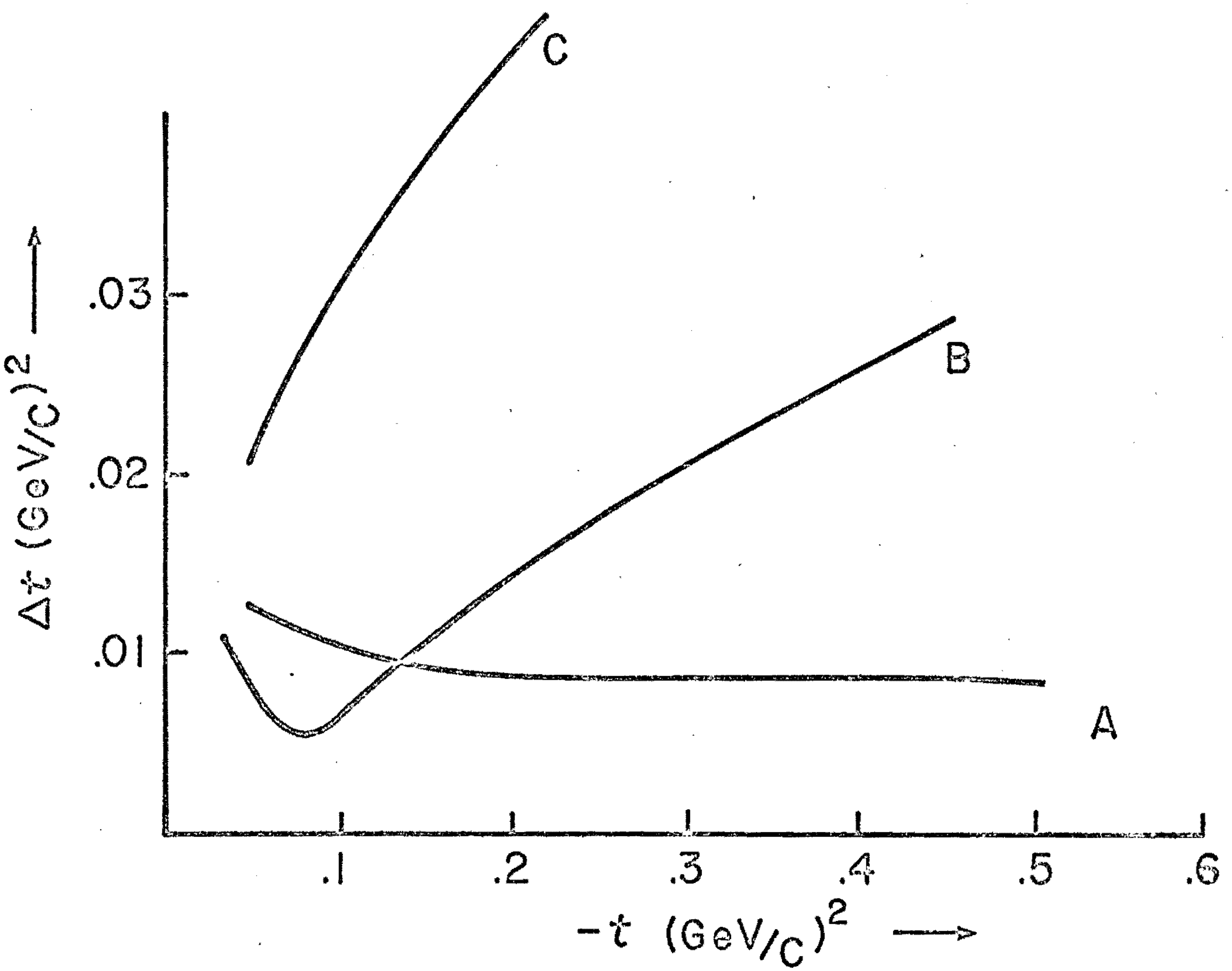

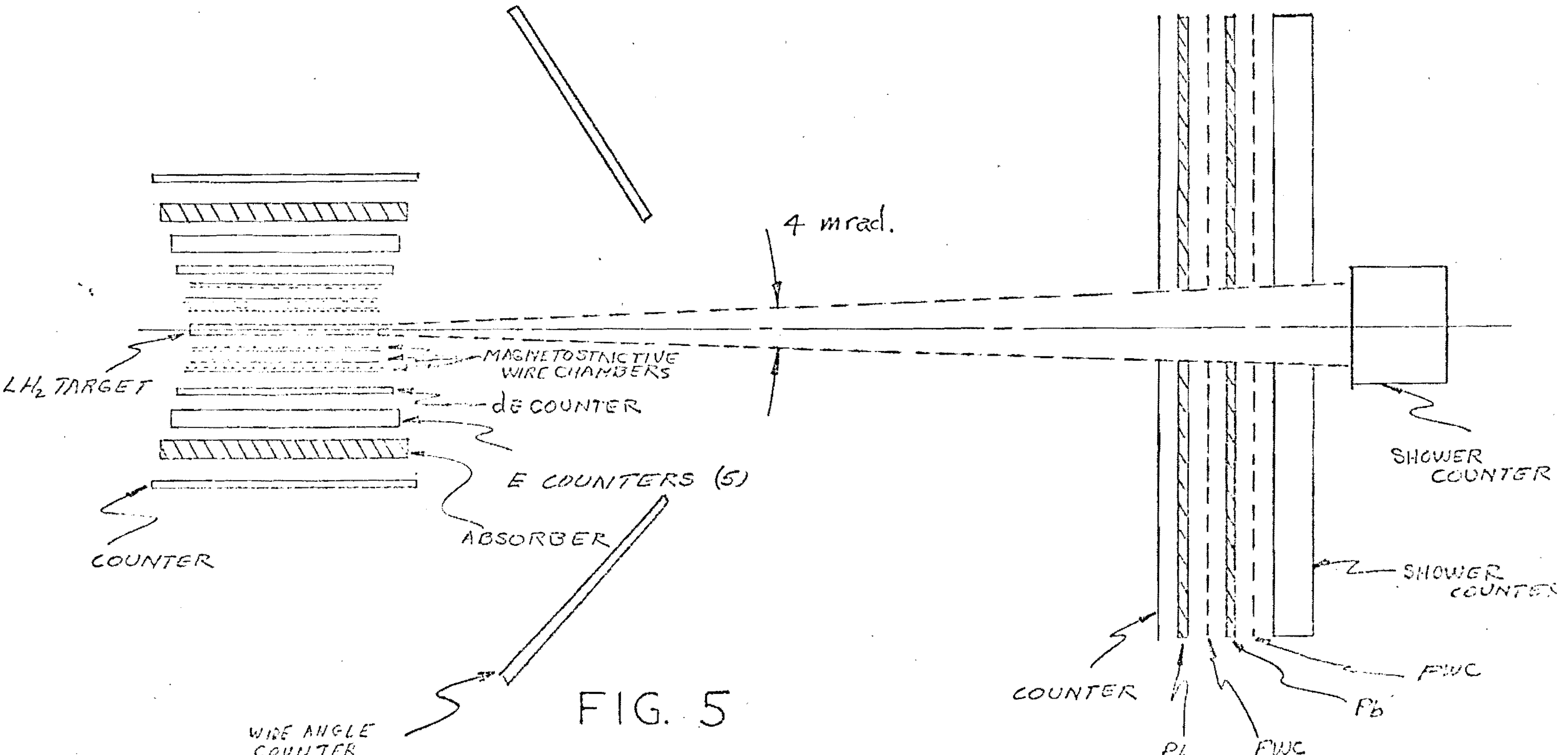

4 mrad.
LH_2 TARGET
MAGNETOSTRICTIVE
WIRE CHAMBERS
dE COUNTER
E COUNTERS (5)
ABSORBER
COUNTER
WIDE ANGLE
COUNTER
SHOWER
COUNTER
SHOWER
COUNTER
COUNTER
Pb
FWC
Pb
FWC

FIG. 5